Modeling the distribution of *Trichodesmium* and nitrogen fixation in the Atlantic Ocean

Raleigh R. Hood and Victoria J. Coles
University of Maryland Center for Environmental Science, Cambridge, Maryland, USA

Douglas G. Capone
Wrigley Institute for Environmental Studies, University of Southern California, Los Angeles, California, USA

Received 18 December 2002; revised 25 February 2004; accepted 17 March 2004; published 4 June 2004.

[1] In this paper we use a coupled, 3-dimensional, biological-physical model, which includes an explicit, dynamic representation of *Trichodesmium*, to predict the distribution of *Trichodesmium* and rates of N_2-fixation in the tropical and subtropical Atlantic Ocean. It is shown that the model reproduces the approximate observed meridional distribution of *Trichodesmium* in the Atlantic and elevated concentrations in specific coastal and open ocean regions where this organism is known to occur. The model also appears to reproduce the observed seasonality of *Trichodesmium* populations at higher latitudes (highest concentrations in summer and fall), but this seasonal cycle may be too pronounced at low latitudes. High and persistent *Trichodesmium* concentrations and rates of N_2-fixation are generated by the model in the Gulf of Guinea off of Africa. This unexpected finding appears to be confirmed by historical measurements. In general, increased *Trichodesmium* concentrations develop in regions where the mixed layer is relatively thin (resulting in high mean light levels) and dissolved inorganic nitrogen (DIN) concentrations and phytoplankton biomass are low for extended periods of time. The model-predicted *Trichodesmium* distributions are therefore very sensitive to the fidelity of the physical model's representation of mixed layer depth variability, and upwelling intensity, and the biological model's estimated DIN and phytoplankton concentrations. The model generates a three-step successional sequence where (1) high DIN concentrations due to upwelling and/or mixing stimulate phytoplankton growth, followed by (2) *Trichodesmium* growth after DIN depletion and phytoplankton decline, followed by (3) enhanced phytoplankton growth due to new nitrogen inputs from N_2-fixation. This sequence develops in response to seasonal variations in mixing in the southwestern North Atlantic and in response to upwelling along the coast of Africa and the equator. We interpret this sequence as representing a diatom- *Trichodesmium*-flagellate succession, which is consistent with observed species successions off of northwest Africa and in the Gulf of Mexico. The results presented in this paper lead us to conclude that our model includes the primary factors that dictate when and where *Trichodesmium* and N_2-fixation occurs in the Atlantic. Moreover, it appears that our model reproduces some of the major effects that diazotrophically-derived inputs of new nitrogen have on the pelagic ecosystem. *INDEX TERMS:* 4815 Oceanography: Biological and Chemical: Ecosystems, structure and dynamics; 4805 Oceanography: Biological and Chemical: Biogeochemical cycles (1615); 4845 Oceanography: Biological and Chemical: Nutrients and nutrient cycling; *KEYWORDS:* nitrogen fixation, Atlantic, *Trichodesmium*

Citation: Hood, R. R., V. J. Coles, and D. G. Capone (2004), Modeling the distribution of *Trichodesmium* and nitrogen fixation in the Atlantic Ocean, *J. Geophys. Res.*, *109*, C06006, doi:10.1029/2002JC001753.

1. Introduction

[2] Recent revised estimates suggest that open ocean N_2-fixation is globally significant, i.e., on the order of 80–110 Tg N yr^{-1} [*Gruber and Sarmiento*, 1997; *Capone et al.*, 1997], and comparable to inputs of NO_3 from the deep ocean in subtropical waters [*Karl et al.*, 1997; *Capone et al.*, 1997, D. G. Capone et al., New nitrogen input to the tropical North Atlantic Ocean by nitrogen fixation by the cyanobacterium, *Trichodesmium spp.*, submitted to *Nature*, 2004 (hereinafter referred to as Capone et al., submitted manuscript, 2004)]. A large fraction of this fixation (perhaps as much as 25%) occurs in the Atlantic Ocean [*Gruber and*

0148-0227/04/2002JC001753$09.00

Sarmiento, 1997; *Capone et al.*, 1997]. We now know that many different diazotrophic organisms contribute to this new nitrogen source [*Hood et al.*, 2000; *Zehr et al.*, 2001]. However, the conspicuous marine cyanobacterium, *Trichodesmium*, is still believed to be the most significant N_2-fixer in the open ocean [*Capone et al.*, 1997, Capone et al., submitted manuscript, 2004]. Although shipboard data are still limited, *Trichodesmium* distributions and rates of N_2-fixation have been better characterized in the Atlantic than in any other ocean basin.

[3] *Trichodesmium* has been the subject of quantitative scientific investigation for nearly a century [see, e.g., *Wille*, 1904; *Dugdale et al.*, 1964; *Carpenter and Capone*, 1992]. The factors that control its growth are thought to include temperature, vertical mixing/light availability, competition with other phytoplankton species, and the availability of iron and/or phosphorus. Temperature control has been inferred from the observation that *Trichodesmium* is not found in significant densities in waters that are colder than 20°C, and rarely blooms below 25°C [*Carpenter and Capone*, 1992; *Capone et al.*, 1997; *Subramaniam et al.*, 2002]. The importance of wind mixing has similarly been deduced from reports that *Trichodesmium* blooms, which develop under calm conditions, dissipate rapidly when winds begin to increase. Accumulations of *Trichodesmium* are rarely observed when it is windy, even when other conditions are favorable for growth [*Capone et al.*, 1997; *Subramaniam et al.*, 2002]. The exact mechanism of this mixing control is not entirely clear. There is undoubtedly some dilution effect that occurs when the mixed layer deepens in response to increased winds, but there is also an impact on the average light in the mixed layer, and therefore the growth rate and physiology of *Trichodesmium* [*Hood et al.*, 2001; *Sañudo-Wilhelmy et al.*, 2001].

[4] *Hood et al.* [2001] hypothesized that, because of it's relatively slow growth rate (3–5 days per doubling [*Capone et al.*, 1997]) and adaptation to high light [*Carpenter et al.*, 1993], *Trichodesmium* concentrations will remain low when dissolved inorganic nitrogen (DIN) is replete in the euphotic zone and/or the mixed layer is thick. Under these conditions, attenuation of light by deep mixing and/or shading by other phytoplankton (which can grow much more rapidly under these conditions) will further reduce the growth rate of *Trichodesmium*, putting it at an even greater disadvantage. According to this hypothesis, *Trichodesmium* can only become dominant when the mixed layer is thin and the growth rate and biomass of other species is restricted by lack of DIN, which provides optimal (high) light conditions for *Trichodesmium* that maximize its growth rate. Regardless of the exact mechanism, it is abundantly clear that mixing strongly influences when and where *Trichodesmium* grows in the open ocean, and that blooms tend to occur where the mixed layer is thin and DIN concentrations are low [*Capone et al.*, 1997; *Hood et al.*, 2001].

[5] Iron and phosphorus may also play significant roles in controlling the distribution and abundance of *Trichodesmium*. Because of the high Fe requirement of the nitrogenase enzyme and the general global correspondence between regions of high iron deposition and high N_2-fixation, it is generally thought that *Trichodesmium* growth is limited by the availability of iron [*Rueter*, 1983; *Rueter et al.*, 1992; *Hood et al.*, 2000; *Berman-Frank et al.*, 2001]. However, the degree to which Fe limits *Trichodesmium* growth in the Atlantic is still an open question. Some studies suggest that it does [*Paerl et al.*, 1994; *Orcutt et al.*, 2001; *Lenes et al.*, 2001; *Walsh and Steidinger*, 2001], while others suggest that it does not [*Sañudo-Wilhelmy et al.*, 2001], and the results from most Fe addition experiments are inconclusive [*Hood et al.*, 2000]. The evidence for phosphorus limitation is also mixed. *Trichodesmium* appears to have a very flexible phosphorus requirement [*Krauk*, 2001], and readily grows [*Carpenter and Romans*, 1991; *Orcutt et al.*, 2001] in waters where the ambient phosphorus concentrations are extremely low (e.g., in the Sargasso Sea [*Wu et al.*, 2000]). Moreover, phosphorus addition assays that have been performed with *Trichodesmium* have not consistently revealed phosphorus limitation [*Hood et al.*, 2000]. However, recent results from the tropical Atlantic suggest that phosphorus is sometimes a limiting factor there [*Sañudo-Wilhelmy et al.*, 2001].

[6] In this paper we model the distribution of *Trichodesmium* and rates of N_2-fixation in the Atlantic using a coupled physical-biological model. Following *Hood et al.* [2001], we hypothesize that *Trichodesmium*'s fundamental physical, chemical, and ecological niche is defined by high light intensity, relatively weak vertical mixing, and low DIN concentrations, where the latter prevents the growth of other, faster growing, phytoplankton species. Further, we implicitly assume that although Fe and P limitation may place constraints upon the total amount of *Trichodesmium* biomass that can develop in any one location, these elements do not dictate when or where *Trichodesmium* occurs. This paper is therefore a test of the *Hood et al.* [2001] hypothesis: We examine the predictions of our model and we determine the degree to which these factors can reproduce observed *Trichodesmium* distributions in the Atlantic. We argue here that changes in mixed layer depth (light) and DIN availability are, in fact, sufficient to explain the large-scale patterns. In addition, the model predicts that *Trichodesmium* and high rates of N_2-fixation should occur in the Gulf of Guinea (off of central West Africa) and that N fluxes due to N_2-fixation should have a significant impact on the distribution of phytoplankton in the open ocean.

2. Coupled Model

[7] The combined model consists of a six-compartment ecosystem model with an explicit representation of *Trichodesmium* coupled to an Atlantic implementation of the Miami Isopycnal Coordinate Model (MICOM). In the following subsections we describe these two models and how they are linked, as well as the forcing, boundary conditions, and parameter choices that were used to generate the solution described and discussed in section 3.

2.1. Ecosystem Model

[8] The biological model (Figure 1) is nitrogen based, and it includes six state variables: dissolved inorganic nitrogen (DIN), dissolved organic nitrogen (DON), phytoplankton (P), detritus (D), heterotrophs (H), and *Trichodesmium* (T). In this model, which is described in detail by *Hood et al.* [2001], *Trichodesmium* is distinguished from phytoplankton by its ability to fix molecular nitrogen (N_2), its slow growth

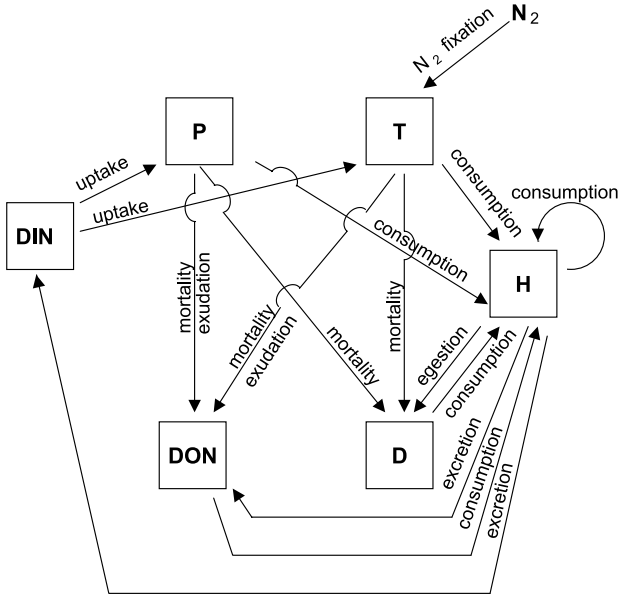

Figure 1. A schematic box diagram of the six-compartment ecosystem model. The state variables are dissolved inorganic nitrogen (DIN), dissolved organic nitrogen (DON), phytoplankton (P), *Trichodesmium* (T), heterotrophs (H), and detritus (D).

rate and its almost complete immunity to heterotrophic (zooplankton) grazing. The growth rate of *Trichodesmium* in this model is entirely determined by light, and therefore also by mixed layer depth and phytoplankton concentrations which both influence the mean light levels in the euphotic zone. There is no Fe or P limitation.

[9] The dual wavelength optical model used by *Hood et al.* [2001] is used here to calculate the average irradiance in each MICOM layer, which is then used to calculate phytoplankton and *Trichodesmium* growth rate. The average light is determined by integrating the irradiance in both wave bands over the layer in question and dividing by layer thickness. In this model, light is attenuated by both phytoplankton and *Trichodesmium* [*Hood et al.*, 2001]. Although the light model includes both shortwave and longwave components, the latter is absorbed rapidly in the surface layer. Thus, for all practical purposes, there is only one band in the photosynthetically active radiation (PAR) range. There is also no feedback between this optical model and the radiative penetration in the physical model, which assumes that all radiation is absorbed in the mixed layer. The detrital sinking flux is calculated using a simple upstream, flux form advection scheme assuming a constant sinking rate.

[10] *Trichodesmium* concentration is reported here in units of colonies/L in order to facilitate intercomparisons between the model estimates and direct measurements. Colony concentrations are calculated from the model-generated *Trichodesmium* mass (mmoles N/m^3) by assuming an average colony nitrogen content of 2 μg N/colony, which is based upon direct measurements from tropical and subtropical western Atlantic waters [*Carpenter*, 1983]. The N_2-fixation rate reported from the model is the net uptake rate of molecular nitrogen by *Trichodesmium*, i.e., the gross nitrogen uptake less any nitrogen taken up from the DIN pool.

2.2. Ecosystem Model Parameter Settings

[11] Except for those discussed below, all of the ecosystem model parameters are set as described by *Hood et al.* [2001, Table 1]. The parameters that are changed include the following: the natural mortality rate of *Trichodesmium* (S_T), the grazing preferences for heterotrophic feeding on T, P, D, H, and DON, (Φ_T, Φ_P, Φ_D, Φ_H, and Φ_{DON}, respectively), and the sinking rate of detritus (w).

[12] The values of S_T and w were re-adjusted following essentially the same procedure as described by *Hood et al.* [2001], except here the model was tuned to simultaneously reproduce satellite-derived, near-surface chlorophyll concentrations throughout the basin, and *Trichodesmium* colony concentrations in the western tropical and subtropical Atlantic. Specifically, this was done by first setting the *Trichodesmium* mortality rate, S_T, to give 1–3 colonies/L between 17°N and 25°N along approximately 57.5°W in October/November. These concentrations are derived from measurements reported by *Carpenter and Romans* [1991], which are generally consistent with the majority of the reports from this region [e.g., *Carpenter and Price*, 1977; *Carpenter and Romans*, 1991; *Sander and Steven*, 1973; *Steven and Glombitza*, 1972; *Dunstan and Hosford*, 1977]. Tuning to the observed *Trichodesmium* concentrations in this manner has the effect of setting the overall concentrations and rates of N_2-fixation throughout the Atlantic basin. However, where and when *Trichodesmium* occurs, and relative concentrations in different ocean regions, are entirely emergent properties of the model.

[13] Once the colony concentrations are set, then w is adjusted to yield seasonal, basin-wide phytoplankton chlorophyll concentrations similar to chlorophyll concentrations derived from composite satellite (SeaWiFS) data. This model fitting is done subjectively and iteratively. The comparison between the model-generated and observed chlorophyll concentrations is described and discussed in detail in section 3.4. Adjusting the sinking rate of detritus in this manner effectively sets the nitrogen export flux so that it balances, on average, the total input of new nitrogen into the upper ocean (i.e., N_2-fixation plus inputs from deep water due to mixing, upwelling and diffusion). The resulting parameter values are $S_T = 0.025\ d^{-1}$ and $w = 6$ m d^{-1}.

[14] In addition, Φ_T was changed from 0 as per *Hood et al.* [2001] to 0.01 in order to add a small amount of density-dependent grazing pressure (negative feedback) on *Trichodesmium*. This change had the effect of generally reducing the high *Trichodesmium* concentrations in the eastern equatorial Atlantic (e.g., in the Gulf of Guinea) which we deemed to be too high in initial model runs relative to concentrations on the western side of the basin. In addition, Φ_P was similarly increased, from 0.25 to 0.3475, to provide stronger grazing pressure and reduce high phytoplankton concentrations in the equatorial upwelling regions. The other three grazing preferences, Φ_D, Φ_H, and Φ_{DON}, were lowered from 0.25 to 0.2175 so that all of the preferences sum to 1.

2.3. General Circulation Model

[15] The 3-D general circulation model is the Miami Isopycnal Coordinate Model (MICOM) [*Bleck and Smith*,

1990; *Bleck et al.*, 1992], whose vertical coordinate is potential density. The model is formulated as a vertical stack of layers, each obeying the shallow water equations and thus having vertically uniform dynamic, thermodynamic, and ultimately ecosystem properties. The uppermost layer is the interface between the atmosphere and the ocean, and acts as a Kraus-Turner bulk mixed layer [*Kraus and Turner*, 1967] with laterally varying thermodynamic properties. Below the mixed layer, advection and diffusion take place along isopycnal surfaces, with diapycnal mixing leading to an explicit exchange of mass and tracers between layers. The diapycnal flux is determined by the difference in concentration between layers and a stratification-dependent diffusion coefficient. In addition, interface smoothing in the model gives rise to isopycnal flux.

[16] For this application, MICOM is configured with a relatively coarse horizontal grid, 2° zonal by 2×cos(lat) mesh. At this resolution, the physical model resolves only the gross features of the ocean gyre systems. Thus we cannot expect to fully resolve the western boundary currents and the equatorial current systems. In addition, this low spatial resolution does not resolve the full spectrum of open ocean eddy variability, which gives rise to low overall eddy kinetic energy [*McGillicuddy and Robinson*, 1997; *McGillicuddy et al.*, 1998; *Mahadevan and Archer*, 2000; *Chassignet and Garraffo*, 2001]. In an exploratory model development effort such as this, the advantage of a low-resolution model is that it allows us to run many (more than 90) iterations of the model for troubleshooting and biological model tuning, which is not feasible with current high-resolution, eddy permitting, and eddy resolving models. The model has 19 layers in the vertical, which are concentrated primarily in the upper ocean and tropical thermocline in order to resolve vertical biological structure and relevant physical processes.

[17] The model domain extends from 45°N to 20°S, 97°W to 13°E. The northern and southern boundaries are outfitted with 5° sponge layers with a tapered relaxation to monthly climatological layer thickness, salinity, and annual mean DIN concentrations from NODC analyzed fields from the Ocean Database 1998 CD-ROM set [*Conkright et al.*, 1998]. The bathymetry is derived from NGDC 5-min gridded bottom topography data ("ETOPO5") by averaging to the model's horizontal grid resolution. This averaged bathymetry resolves only major topographic features and shelf areas within the model domain. Islands are not fully resolved, for example, the Antilles Archipelago is represented as a shoal region extending up to about 2000 m depth. Vertical diffusion is implemented with a Nyquist frequency dependent mass transfer. Isopycnal diffusion of tracer quantities is set at 0.5 cm s^{-1} × the grid size, or 1. × 10^7 cm^2 s^{-1}. In MICOM, horizontal advection of salt and biological tracers is carried out using an upstream advection scheme which corrects for numerical diffusion [*Smolarkiewicz*, 1983].

[18] The model is forced using surface wind stress and speed, and air temperature and humidity from the COADS climatology [*da Silva et al.*, 1994]. Precipitation and surface radiation are derived from the Oberhuber atlas [*da Silva et al.*, 1994]. The radiation data from the latter (which provides daily averaged values with both long and shortwave components) are also used to specify the surface irradiance for the dual wavelength optical model that calculates the subsurface irradiance for the ecosystem model. River runoff is prescribed seasonally as an augmentation of the precipitation field for four freshwater sources: the Amazon, the Congo, the Orinocco, and the Mississippi. The flows are taken from *Carton* [1991]. Currently, these rivers do not act as sources of nutrients to the model ocean.

3. Results and Discussion

[19] In this section we discuss our main run solution, which was derived using the tuning procedure described in section 2.2, and we validate it against physical, chemical, and biological observations. In section 3.1 we compare the model-estimated mixed layer depth variability to seasonal climatological fields, and we describe how this influences the average light in the mixed layer. In section 3.2 we validate the modeled *Trichodesmium* distributions against all available direct measurements of *Trichodesmium* biomass. In section 3.3 we compare model-generated, meridional DIN sections with seasonal climatological DIN data from the World Ocean Database 1998 CD-ROM set [*Conkright et al.*, 1998], and in section 3.4 we compare modeled phytoplankton concentrations in the mixed layer with SeaWiFS-derived near surface chlorophyll estimates. Finally, we conclude the results and discussion with section 3.5, where we describe the model-generated seasonality in *Trichodesmium*, phytoplankton, and DON concentrations along two meridional sections, focusing on successional patterns generated by the model.

3.1. Mixed Layer Depth and Light

[20] Proper representation of mixed layer depth (MLD) and its variability are crucial for modeling phytoplankton and *Trichodesmium* concentrations in the Atlantic (and in the ocean in general [*McCreary et al.*, 1996, 2001; *Hood et al.*, 2001, 2003]), because the MLD has a large impact upon the light and nutrient levels that are experienced by the autotrophs in the system. Shallow mixed layers generated by surface heating and detrainment tend to result in low nutrient and high light conditions, whereas deep mixed layers generated by surface cooling and entrainment give rise to the opposite. As discussed above, in our ecosystem model the latter will tend to lead to phytoplankton dominance in the mixed layer, whereas prolonged periods of the former will eventually allow *Trichodesmium* populations to increase near the surface.

[21] However, MLD can also be strongly influenced by upwelling and downwelling, which can lead to very different light and nutrient conditions. If the mixed layer in MICOM is at its minimum thickness (20 m), upwelling can inject nutrients into the surface layer which will result in a high light (thin mixed layer) and high nutrient condition. These circumstances will tend to arise in regions where there is continuous upwelling and strong subsurface stratification, such as the equator. In contrast, if the mixed layer deepens due to convergence of nutrient-depleted surface waters, then it can result in a low light and low nutrient condition. These circumstances will tend to arise in regions where there is continuous convergence, such as the central gyres. Thin mixed layers associated with continuous upwelling provide optimal light and nutrient conditions for phytoplankton growth in our ecosystem model, and there-

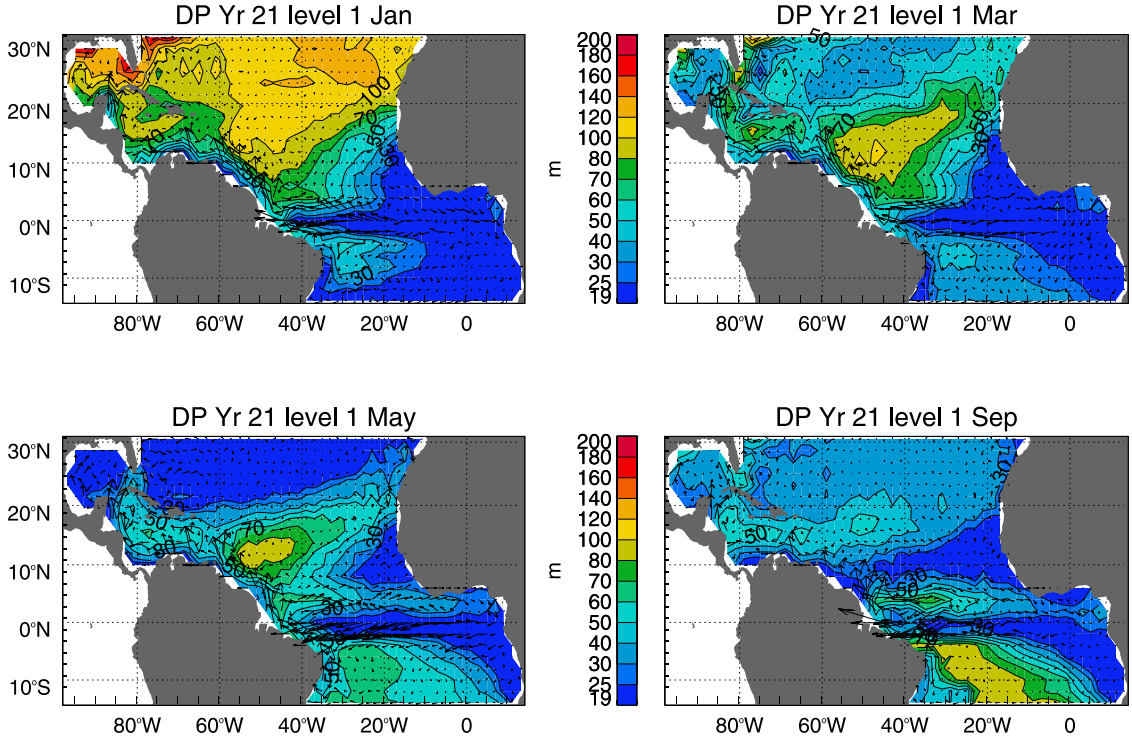

Figure 2. Seasonal MICOM-simulated mixed layer depth in meters (color contours) and horizontal velocity in relative units (vectors). Each panel is the average of two instantaneous fields from the middle of two months. Jan, January/February; Mar, March/April; May, May/June; Sep, September/October. The mixed layer depth here is synonymous with the thickness of the surface layer in the model.

fore tend to result in phytoplankton dominance and low *Trichodesmium* concentrations. Thicker mixed layers associated with convergence and downwelling can result in conditions more favorable for *Trichodesmium* growth in our model, but these favorable conditions are ephemeral; that is, as the mixed layer deepens, increased light limitation progressively limits *Trichodesmium* growth.

[22] In the MLD analyses that follow we compare MLD variability generated by the model (Figure 2) with MLD estimated from monthly climatological temperature and salinity from NODC analyzed fields from the World Ocean Database 1998 CD-ROM set [*Conkright et al.*, 1998] (Figure 3). Recall that MICOM estimates MLD using a Kraus-Turner-like model. Thus the two criteria are very different, but the patterns should be similar. The modeled light fields, however, are synoptic (Figure 4) to facilitate comparisons with the synoptic model output described in later sections.

[23] The modeled and observed patterns in MLD variability are basically similar at lower latitudes in winter (February), i.e., shallow MLDs along the northern coast of South America, in the Cape Verde/Sierra Leone region, and all along the coast of Africa in the Gulf of Guinea and southward (Figures 2 and 3). The model also reproduces the shallow mixed layers that are observed along the equator. However, in winter the model mixes too deeply (>100 m) at higher latitudes in the North Atlantic. Note in particular that the modeled mixed layer is much too deep (>100 m) in winter in the northern Gulf of Mexico and along the coast of Florida, and 20–30 m too deep throughout the Caribbean Sea.

[24] The relatively deep mixing generated by the model at higher latitudes in the Northern Hemisphere winter results in low mean light conditions (<10 W/m^2) over much of the central and eastern North Atlantic (Figure 4). In contrast, the shallow MLDs (20 m) off of the North coast of South America and over large areas along the equator and off of Africa south of 10°N result in relatively high light conditions (>30 W/m^2).

[25] In spring the MLDs in the model between 20°N and 30°N are shallower than observed (Figures 2 and 3) over much of the North Atlantic (<60 m). Although the pattern of MLD variability generated by the model is still essentially similar to the observations at low latitudes, there are some significant discrepancies. For example, the data reveal much more extensive shallow mixed layers all along the northern coast of South America compared to the model. Note also that in the model the MLDs are considerably deeper and extend over a broader area between the northeastern coast of Brazil and northwest Africa.

[26] Because of the shallow MLDs, the mean light levels in the model increase (to >20 W/m^2) over much of the subtropical North Atlantic (including the Gulf of Mexico and Caribbean waters) in spring (Figure 4). However, the light levels remain relatively low (<20 W/m^2) where the MLDs are deep in the center of the basin between 5°N and 25°N, and along the coast in the Gulf of Mexico, off of Florida, and in places along the coast of Central America. The light levels in the mixed layer off of the north coast of South America and over large areas along the equator and off of Africa remain relatively high (>35 W/m^2).

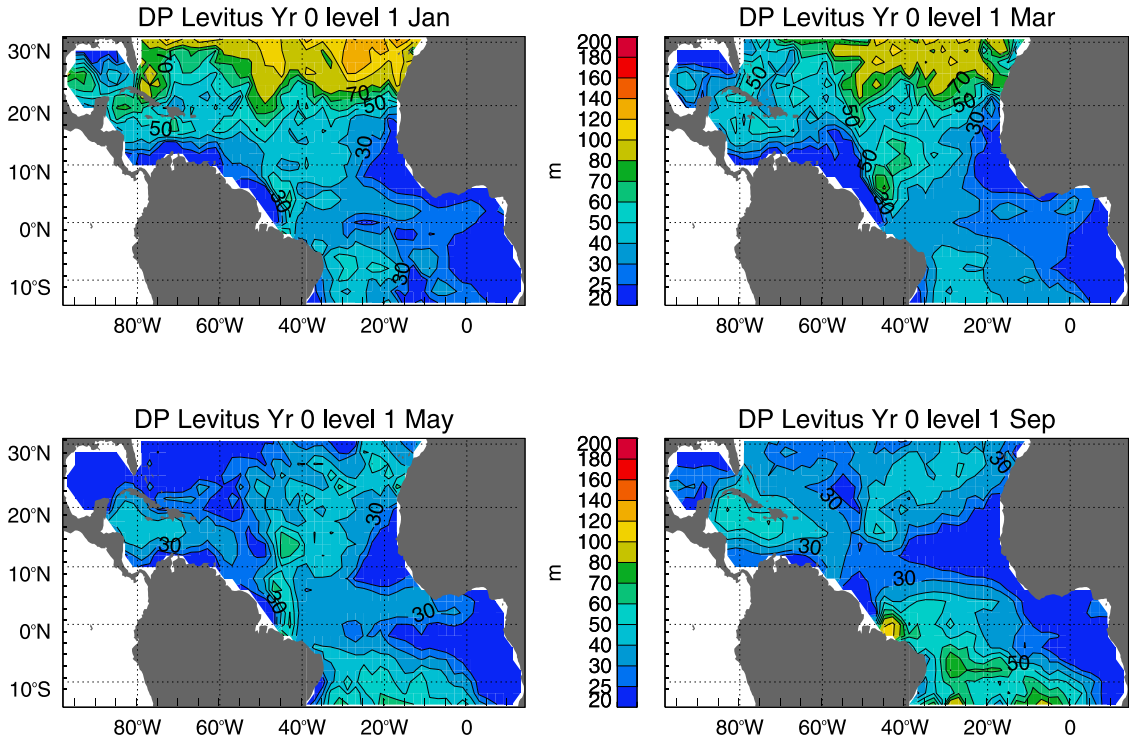

Figure 3. Seasonal mixed layer depth in meters calculated from monthly salinity and temperature climatologies from NODC analyzed fields from the World Ocean Database 1998 CD-ROM set [*Conkright et al.*, 1998]. Each panel is the average of two climatologies for the specified months. Jan, January/February; Mar, March/April; May, May/June; Sep, September/October. MLD was estimated using a simple $\Delta\sigma_\theta = 0.01$ criterion (i.e., MLD is taken to be the depth where σ_θ exceeds the surface value by 0.01 units).

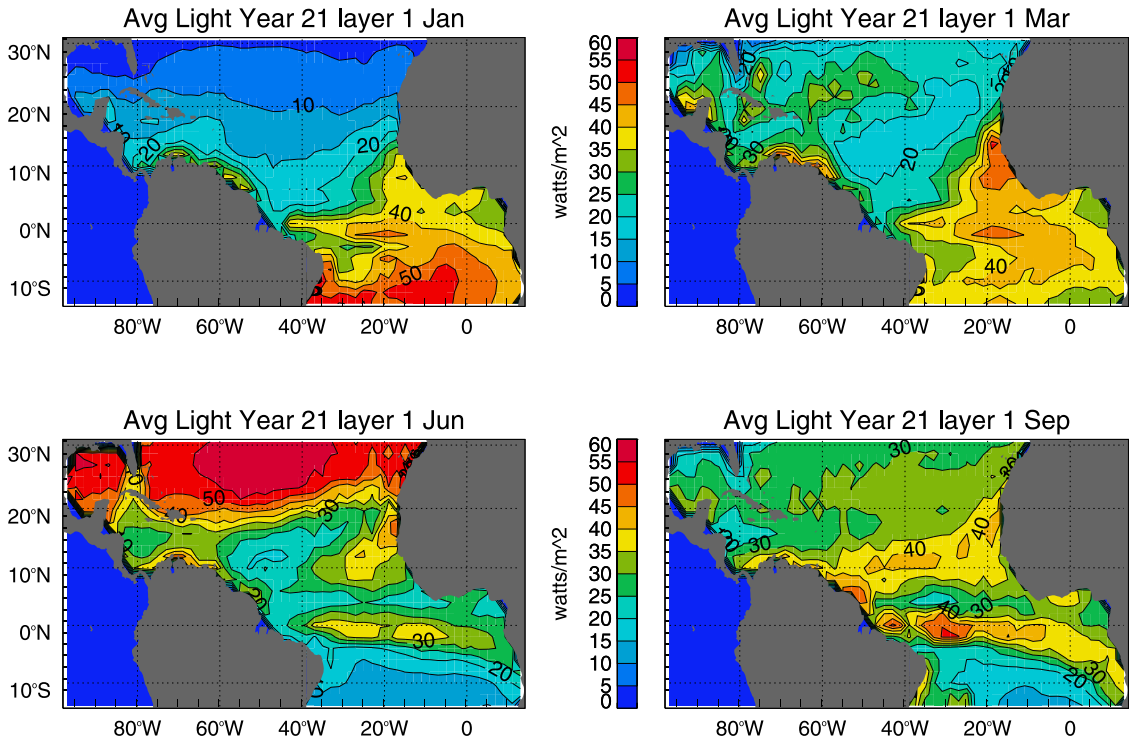

Figure 4. Daily average light averaged over the mixed layer in Watts m^{-2} as a function of season from the model. Here the fields are synoptic, taken from the middle of the specified month.

Table 1. Observed *Trichodesmium* Concentrations in Atlantic Waters

Number	Location	Dates	Observed Concentration	Reference
		Gulf of Mexico, South Atlantic Bight		
1	northwest Gulf of Mexico (27°N, 95°W)	24–28 July 2000	2–5 col/L, 51 col/L at 1 sta.	*Krauk* [2001]
2	northwest Gulf of Mexico	summer	10–20 col/L ("typical")	T. Villareal (personal communication, 2002)
3	northwest Gulf of Mexico	Dec 2000	0 col/L	T. Villareal (personal communication, 2002)
4	southwest Florida coast (27°N, 83.5°W)	June–Sept. 1999	2–22 col/L (max. in June)	*Lenes et al.* [2001]
5	southwest Florida coast (26.75°N, 82.5°W)	July 1980	125 col/L[a]	*Walsh and Steidinger* [2001]
6	southwest Florida coast (25.5°N–29°N, 81.5°W–83°W)	multiyear time series	0.5–50 col/L[b] (most summer/fall)	*Walsh and Steidinger* [2001]
7	South Atlantic Bight (29°N, 80°W)	30 Oct. 1998	20–150 col/L[c]	*Subramaniam et al.* [2002]
8	South Atlantic Bight (30°N–33°N, 78°W–81.5°W)	Sept. 1973 to July 1974	0–>5 col/L[a] (present all year)	*Dunstan and Hosford* [1977]
		Sargasso Sea, Carribbean, Northern Coast of South America		
9	northwest Atlantic 10°N–18°N along ≈60°W	Oct.–Nov. 1990	1 col/L	*Carpenter and Romans* [1991]
10	northwest Atlantic 18°N–23°N along ≈60°W	Oct.–Nov. 1990	1–3 col/L	*Carpenter and Romans* [1991]
11	northwest Atlantic 23°N–32°N along ≈60°W	Oct.–Nov. 1990	0.5–1.5 col/L	*Carpenter and Romans* [1991]
12	northwest Atlantic 11.5°N–16.5 °N, 57°W–62°W	Feb. 1961	3–11 col/L[a]	*Hulburt* [1962]
13	northwest Atlantic 16.5°N–30°N, 48°W–57°W	Feb. 1961	0–0.6 col/L[a]	*Hulburt* [1962]
14	southwest Carribbean coastal waters-Central Carribbean Sea	Nov. 1965	0.15–4.5 col/L[a]	*Hulburt* [1968]
15	north Sargasso Sea 26°N–28°N, 61.5°W–64.5°W	Sept. 1994	0.05–0.25 col/L	*Orcutt et al.* [2001]
16	north Sargasso Sea 28°N–33°N, 61.5°W–64.5°W	Sept. 1994	<0.025 col/L	*Orcutt et al.* [2001]
17	north Sargasso Sea 29°N–35°N, 66.7°W–61.1°W	July 1995	<0.025 col/L	*Orcutt et al.* [2001]
18	east Carribbean Waters 10°N–20°N, 62°W–76°W (multicruise average)	Feb.–March, Aug. 1974	1–4 col/L[b]	*Carpenter and Price* [1977]
19	Sargasso Seawaters (multicruise average)	Sept.–Oct. 1973, Aug. 74	0.25–0.5 col/L[b]	*Carpenter and Price* [1977]
20	north Carribbean (17.6°N, 66.9°W)	May 1995 to May 1996	0.003–0.014 col/L	*Navarro* [1998]
21	north Carribbean (17.6°N, 66.9°W)	Jul–Oct 1996	0.014–0.5 col/L	*Navarro* [1998]
22	north Carribbean (17.6°N, 66.9°W)	Nov. 1996 to Sept. 1997	0.001–0.007 col/L	*Navarro* [1998]
23	north Carribbean (17.6°N, 66.9°W)	Oct–Nov 1997	0.003–0.03 col/L	*Navarro* [1998]
24	east of Puerto Rico and vicinity (14°N–20°N, 70°W–50°W)	May–June 1994	5–25 col/L[a]	*Carpenter et al.* [2004]
25	east of Puerto Rico and vicinity (14°N–20°N, 65°W–50°W)	Oct.–Nov. 1996	0.5–1.5 col/L[a]	*Carpenter et al.* [2004]
26	east of Puerto Rico and vicinity (20°N–25°N, 70°W–60°W)	Oct.–Nov. 1996	0.5–3 col/L[a]	*Carpenter et al.* [2004]
27	east of Barbados (13°N, 59°W)	Aug. 1967 to June 1970	0–10 col/L[a] (3 mo. oscill.)	*Steven and Glombitza* [1972]
28	east of Barbados (13°N, 59°W)	multiyear time series	0–10 col/L[a] (3 mo. oscill.)	*Borstad* [1982]
		Eastern, Northeastern Coast of Brazil, Offshore Waters		
29	east Coast of Brazil (5°S–15°S, 25°W–35°W)	Sept.–Oct.	0 col/L	*Tyrrell et al.* [2003]
30	northeast coast of South America (14°N, 55°W)	March–April 1996	1–8 col/L[a]	*Carpenter et al.* [2004]
31	northeast coast of South America offshore waters (0°N–8°N, 30°W–45°W)	March–April 1996	1–8 col/L[a]	*Carpenter et al.* [2004]
32	northeast coast of South America, primarily Amazon outflow (0°–24°N, 45°W–66°W)	Nov. 1964	1–9 col/L[d], 117 col/L[d] at 1 sta.	*Goering et al.* [1966]

Table 1. (continued)

Number	Location	Dates	Observed Concentration	Reference
33	northeast coast of South America, primarily Amazon outflow (0°–24°N, 45°W–66°W)	May 1965	1–13 col/L[d]	*Goering et al.* [1966][e]
34	northeast coast of South America and offshore waters (7°N–14°N, 42°W–55°W)	Oct. 1996	1–4 col/L[a]	*Carpenter et al.* [2004]
		Northwest African Coast, Equatorial Waters		
35	northwest Africa coastal waters (18°N–24°N, 16°W–22°W)	Nov. 1975	17–407 mm/cm^2 [f]	*Vallespinos* [1985]
36	northwest Africa coastal waters (18°N–24°N, 16°W–22°W)	spring	0 col/L	*Vallespinos* [1985]
37	northwest Africa coastal waters (16°N–22°N, 16°W–22°W)	Aug. 1971	30–5308 mm/cm^2 [f]	*Margalef* [1973]
38	northwest Africa offshore waters (22°N, 30°W–45°W)	Aug.–Sept. 1989	>0 col/L	*Hernańndez-León et al.* [1999]
39	northwest Africa offshore waters (20°N–30°N, 20°W)	Sept.–Oct.	0–10 col/L[a]	*Tyrrell et al.* [2003]
40	northwest Africa offshore waters (15°N–20°N, 20°W–25°W)	Sept.–Oct.	<1 col/L[a]	*Tyrrell et al.* [2003]
41	Sierra Leone coastal waters (7°N–10°N, 10°W–15°W)	Dec.–April	>0 col/L	*Aleem* [1980]
42	northwest Africa/Sierra Leone, North Equatorial Waters (3°N–15°N, 10°W–25°W)	Sept.–Oct.	0–>100 col/L[a]	*Tyrrell et al.* [2003]
43	Open Ocean Equatorial Waters (10°S–3°N, 10°W–25°W)	Sept.–Oct.	<1 col/L[a]	*Tyrrell et al.* [2003]
44	Open Ocean Equatorial Waters (2°S–3°N, 22°W)	Feb.–March 1979	0 col/L	*Bauerfeind* [1987]
45	Open Ocean Equatorial Waters (2°S–3°N, 22° W)	April 1979	>0 col/L	*Bauerfeind* [1987]
46	Open Ocean Equatorial Waters (2°S–3°N, 22°W)	May–June 1979	1–8.5 col/L[g]	*Bauerfeind et al.* [1983]
		Gulf of Guinea, West African Coastal Waters		
47	Gulf of Guinea (25- to 200-m shelf waters off Abidjan ≈2°W–8°W)	3-year time series	>0 col/L	*Dandonneau* [1971]
48	west African coastal waters (off Angola 11°S, 4°E)	April 1968	≈1 col/L[h]	*An* [1971]
49	west African Coastal Waters (off Angola 14°S, 8°E–5°W)	April 1968	≈0.0002 col/L[h]	*An* [1971]
50	Open Ocean Waters off of West Africa (5°S–15°S, 10°E–0°)	Sept.–Oct.	0 col/L[a]	*Tyrrell et al.* [2003]

[a]Calculated from filament concentrations assuming 200 filaments per colony.
[b]Calculated from cell concentrations assuming 100 cells per filament and 200 filaments per colony.
[c]Calculated assuming 20–50 ng Chla per colony.
[d]Calculated from nitrogen concentrations assuming 2 μg N per colony.
[e]See also *Calef and Grice* [1966].
[f]Published unit that could not be converted to col/L.
[g]Calculated from total chlorophyll concentration using variable percent cyanobacterial chlorophyll provided by E. Carpenter, and assuming 20–50 ng Chla per colony.
[h]Calculated from total cell concentrations using specified cyanobacterial fractions and assuming 100 cells per filament and 200 filaments per colony.

[27] The agreement between the modeled and observed MLDs is probably best in summer (June) and fall (September) (Figures 2 and 3). The model reproduces all of the observed shallow regions during these time periods, though not in precise detail. The model also generates deeper MLDs in June and September in the Southern Hemisphere, and a band of relatively deep MLDs extending zonally between 10°N and 25°N, as observed. Note, however, that the shallow MLDs along the equator, which are associated with equatorial upwelling, extend too far to the west in the model compared to the observations. This discrepancy arises due to the relatively low resolution of the model, which results in overestimation of the strength and extent of equatorial upwelling.

[28] Figure 4 shows that the average light in the mixed layer is relatively high in all of the regions where the mixed layer is shallow. In summer (June) the light levels are actually higher (>45 W/m^{-2}) north of 20°N (in the open ocean and in the Gulf of Mexico) than in the coastal and open ocean upwelling regions, even though the mixed layer is at its minimum thickness in both. This happens because phytoplankton concentrations are much higher in the upwelling areas which results in more rapid light attenuation (see Figure 12 in section 3.4).

3.2. Observed *Trichodesmium* and Rates of N_2-Fixation

[29] In this section we compile and summarize the available direct measurements of *Trichodesmium* biomass

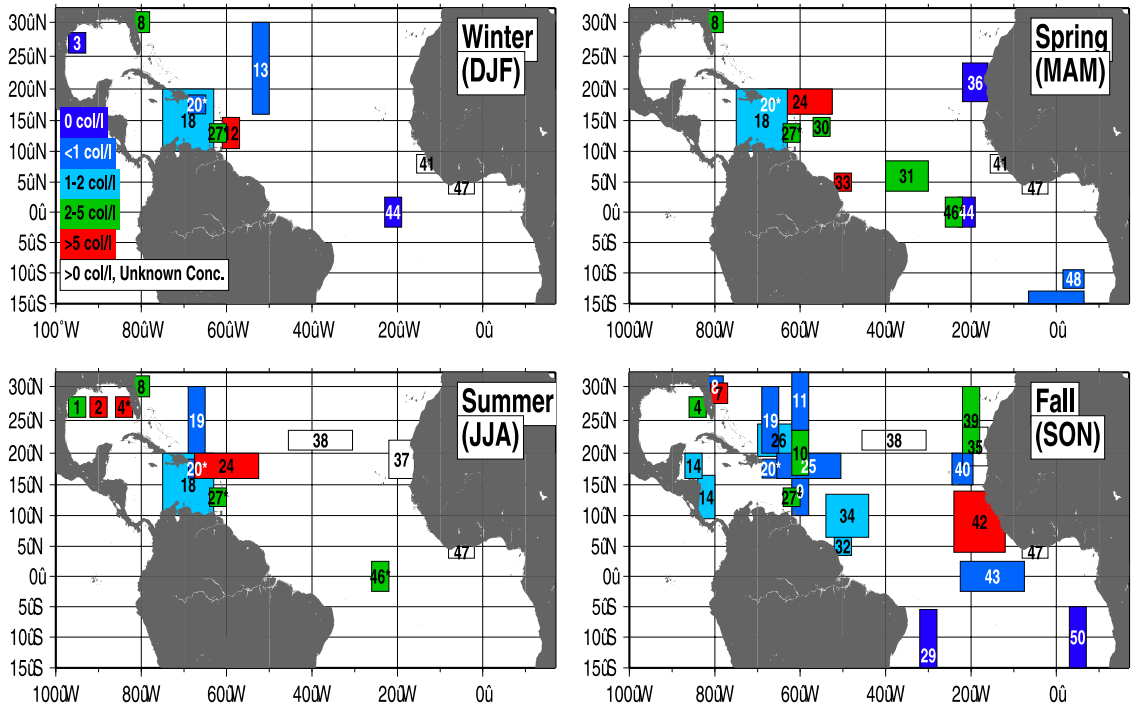

Figure 5. Observed *Trichodesmium* concentrations in the Atlantic as a function of season from Table 1. Concentrations, which are expressed in colonies/liter, are divided into six broad concentration categories as specified by the color bars in the top left panel. The areas specified are intended to crudely represent the regions where the observations were collected. The references marked with asterisks relate to multiple observations in Table 1, i.e., 4* = 4, 5, 20* = 20–23, 27* = 27, 28 and 46* = 45, 46. See Table 1 for details on specific concentrations, unit conversions, and literature sources.

from the Atlantic between 30°N and 15°S, and compare them to the model-generated *Trichodesmium* concentrations. The measurements are reported in Table 1 along with the specific conversion factors that were applied to each data source to convert them to common units of colonies/L (see footnotes in Table 1). We also use this information to generate a crude seasonal/spatial map of *Trichodesmium* biomass (Figure 5) that directly compares the observed and modeled concentrations. Direct N_2-fixation rate estimates are also available (and discussed below) in some cases, but the focus here is on biomass rather than the rates because there are many more biomass measurements.

[30] Figure 5 reveals that the measurements are very patchy in both space and time, and Table 1 shows that only a few time series exist. There are also far more measurements in the western Atlantic (especially the Caribbean). Moreover, comparisons with the model are confounded to some degree by the fact that surface accumulations of *Trichodesmium* populations often develop under stratified conditions in the field, which can give rise to extremely high measured concentrations which cannot be replicated by the model because it averages the concentrations over the minimum MICOM MLD of 20 m. We point out where these kinds of effects may be important.

3.2.1. Meridional and Zonal Extent of *Trichodesmium* and N_2-Fixation

[31] The meridional extent of the *Trichodesmium* populations and rates of N_2-fixation predicted by the model are essentially correct (Figures 6 and 7); that is, the model generates *Trichodesmium* distributions that are largely confined to tropical and subtropical waters as observed [*Carpenter*, 1983; *Capone et al.*, 1997]. Although it has often been assumed that the northern extent of *Trichodesmium* populations is dictated by temperature (kinetic) control of their growth rate [*Carpenter*, 1983; *Carpenter and Capone*, 1992; *Moore et al.*, 2002], our model does not require this mechanism to reproduce the observed range. Rather, variations in *Trichodesmium* biomass and rates of N_2-fixation in the model are determined primarily by the depth and duration of winter mixing. At higher latitudes, deeper winter mixing results in lower light levels and higher DIN concentrations which favor phytoplankton growth. At lower latitudes, persistent net surface heating results in thinner mixed layers, higher mean light levels, and DIN depletion, which favors *Trichodesmium* growth. This dynamic in the model is consistent with recent observations which show that there is a strong correlation between MLD and N_2-fixation rate in situ [*Sañudo-Wilhelmy et al.*, 2001].

3.2.2. Spatial Pattern and Seasonality in the Gulf of Mexico and the South Atlantic Bight

[32] *Trichodesmium* is commonly observed and highly variable in the Gulf of Mexico, with most accounts from summer and fall. Concentrations of 10–20 colonies/L are often observed in northwestern Gulf waters in summer, whereas they appear to be absent in winter (T. Villareal, personal communication, 2002). *Krauk* [2001], for example, observed typical concentrations of 2–5 colonies/L in the northwestern Gulf in late July (24–28, 2000), but at one station concentrations were an order of magnitude higher. In the eastern Gulf off of the west coast of Florida,

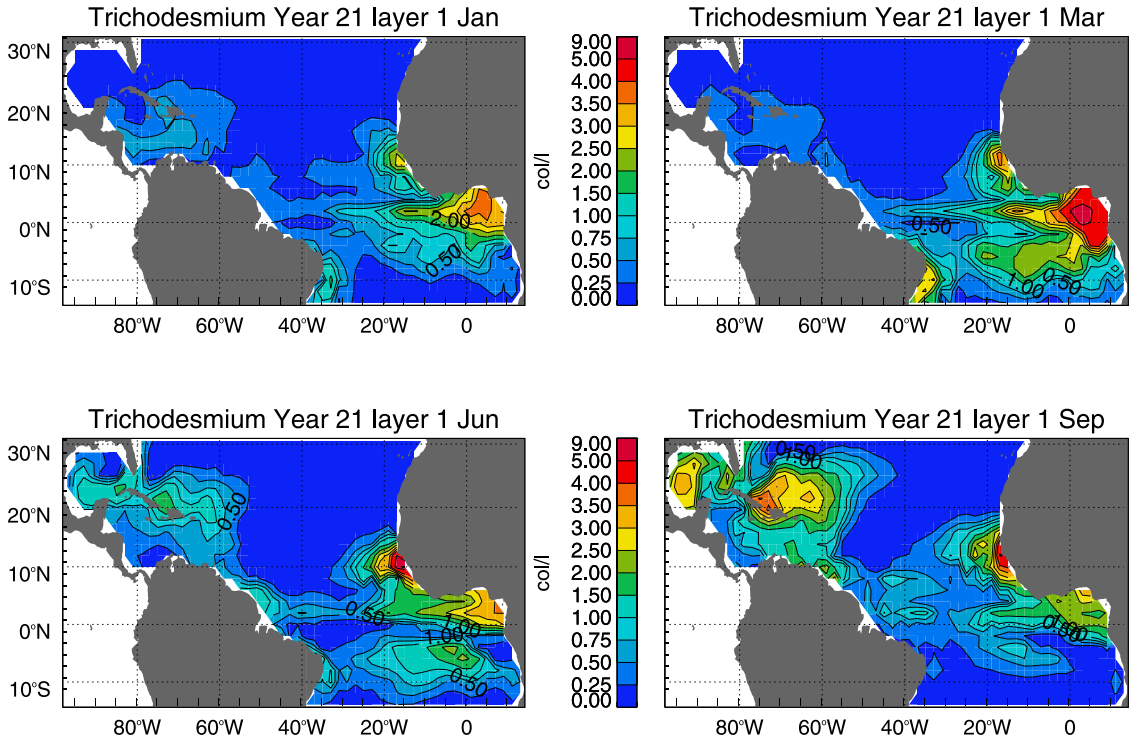

Figure 6. Model-estimated *Trichodesmium* concentration in the mixed layer as a function of season. The fields are synoptic, from the middle of the specified month. *Trichodesmium* biomass is expressed in colonies/liter, which was converted from nitrogen biomass assuming 2 μg N per colony.

Lenes et al. [2001] measured concentrations ranging from 2 to 22 colonies/L in surveys in June through September, with the maximum occurring in early July (1999). *Walsh and Steidinger* [2001] report a mean concentration of 125 colonies/L in a bloom in early July (1980) in the same general area. An historical time series of *Trichodesmium* concentration measurements constructed by *Walsh and Steidinger* [2001] reveals that blooms typically develop

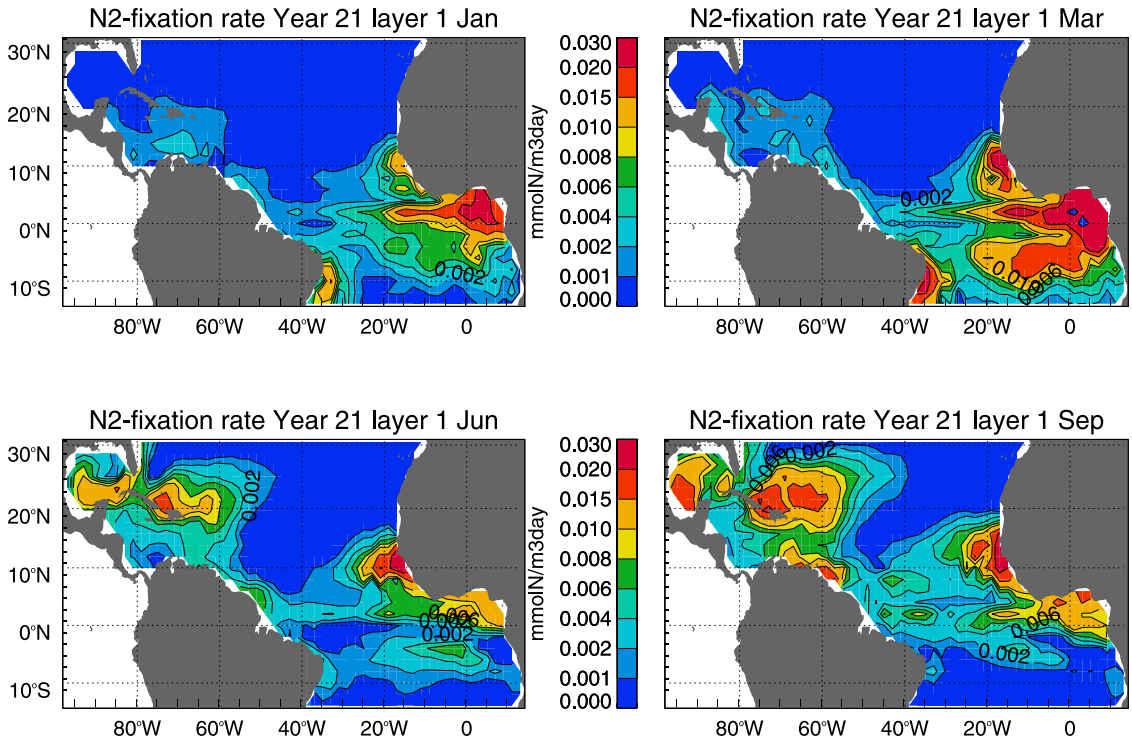

Figure 7. Model-estimated nitrogen fixation rate in the mixed layer as a function of season. The fields are synoptic, from the middle of the specified month. The rates are expressed in mmoles N m^{-3} day^{-1}).

off the west coast of Florida in summer and fall, with concentrations varying between 0.5 and 50 colonies/L. However, this time series also shows several instances of bloom development in winter and spring. Lenes et al. and Walsh and Steidinger link bloom development to Fe deposition events.

[33] *Trichodesmium* blooms also develop in the South Atlantic Bight (SAB) along the southeastern coast of the United States, with high concentrations most often in summer and fall. For example, using satellite remote sensing techniques, *Subramaniam et al.* [2002] estimated *Trichodesmium* specific chlorophyll concentrations up to 3 mg m^{-3} in a coastal bloom off of Florida in October, which is equivalent to 20 –150 colonies/L. However, *Dunstan and Hosford* [1977] reported significant concentrations (>5 colonies/L) in spring, as well as in summer and fall.

[34] Figure 6 shows that the model predicts *Trichodesmium* concentrations of 1–3.5 colonies/L, which develop in summer and fall along the coasts in the Gulf of Mexico and the SAB, and very low concentrations in winter and spring. Note the development of two distinct patches in the Gulf in September: one off of southwest Florida and another dominating the western half of the region. These locations are consistent with the observations, and the concentrations are comparable to the observed "background" *Trichodesmium* concentrations in these waters. We speculate that the higher observed concentrations are associated with surface accumulations that develop in warm, stratified waters. As we mentioned above, our model cannot reproduce these conditions. We can, however, estimate what the model concentrations would be if it could: If the maximum model-generated mixed layer concentrations of 1–3.5 colonies/L in a 20-m MLD are concentrated in a layer 1 m thick, it would give 20–70 colonies/L, which is consistent with most of the higher measured concentrations in the Gulf and the SAB.

[35] The seasonality generated by the model is also generally consistent with the observed seasonal patterns. However, it appears that *Trichodesmium* blooms sometimes develop in the winter and spring in the Gulf and in the SAB (*Walsh and Steidinger* [2001] and *Dunstan and Hosford* [1977], respectively), which is not consistent with the model. This discrepancy may be due to the fact that the model substantially overestimates MLD in these waters in winter and spring, which would prohibit the development of *Trichodesmium* blooms during these seasons, and delay the onset of population increases in the summer. We also suggest that while blooms may occasionally develop in the winter and spring in the Gulf and SAB, this is probably unusual.

[36] Although *Lenes et al.* [2001] and *Walsh and Steidinger* [2001] attribute the *Trichodesmium* blooms off of the west coast of Florida to Fe deposition events, no such mechanism exists in our model; that is, the high concentrations that develop in the model in summer and fall are linked to stratification, increased light in the mixed layer, and depleted DIN concentrations, not Fe deposition. We believe that thin MLD and depleted DIN conditions are the first-order controls on *Trichodesmium* growth and therefore must be satisfied first for *Trichodesmium* to grow. However, it is also possible that the converse is true; that is, even if these physical conditions are met, a bloom may not develop in the absence of significant atmospheric Fe deposition.

3.2.3. Spatial Pattern and Seasonality in the Sargasso Sea, Caribbean, and the Northern Coast of South America

[37] Although numerous observations have been made of *Trichodesmium* in the Sargasso Sea and Caribbean waters over the last 20 years, these measurements are still very patchy in both space and time, and the concentrations vary tremendously. *Carpenter and Romans* [1991] reported surface concentrations along a transect from Barbados to Bermuda in October/November. These data show about 1 colony/L between 10°N and 18°N, increasing to as much as 3 colonies/L between 18°N and 23°N, and then decreasing again to 1 colony/L or less approaching Bermuda. Comparison with the model results for September reveals essentially the same meridional pattern, with similar concentrations (Figure 6). Although the model was tuned to reproduce these observations between 18°N and 23°N, it was not tuned to reproduce the observed meridional pattern, which it does remarkably well.

[38] *Hulburt* [1962] published a February transect extending northeastward from Barbados to approximately 30°N, 48°W. North of 16°N they encountered *Trichodesmium* at only one station location, but southward of this location they measured individual filament concentrations equivalent to 5–10 colonies/L. Comparison with the model reveals essentially the same pattern, but with much lower concentrations, increasing to only about 0.5 colonies/L in the vicinity of Barbados. In another transect in the southwestern Caribbean Sea (running along the coast from the Panama Canal up along the coast of Nicaragua into the northern Caribbean), *Hulburt* [1968] measured highly variable concentrations ranging from 0.150 to 4.5 colonies/L in early November (1965). The model predicts somewhat lower concentrations in this region in September, ranging from 0.25 to 0.75 colonies/L. As discussed above, the model overestimates the MLD throughout much of the Caribbean in winter and spring, which may lead to underestimation of *Trichodesmium* concentrations all year round (see also section 3.3.4).

[39] More recently, *Orcutt et al.* [2001] measured colony concentrations along a transect near Bermuda in September of 1994 (between 26°N and 33°N) and July of 1995 (between 29°N and 35°N). Both transects show low *Trichodesmium* concentrations near Bermuda (0–0.025 colonies/L) with values increasing southward in September of 1994 to 0.250 colonies/L at 26°N. These observations are also consistent with the model, which predicts low concentrations near Bermuda all year round, and dramatic increases in colony concentrations just south of Bermuda (between 25°N and 30°N) in September. Although the model-estimated concentrations at 26°N are higher than observed (1–2 colonies/L estimated versus 0.250 colonies/L observed), *Orcutt et al.* [2001] reported that a large fraction (up to 90% of the population) existed as free trichomes. If this is taken into account, then the observed *Trichodesmium* biomass at 26°N is roughly consistent with the model.

[40] Finally, compiling data from three broad area cruises in the Caribbean and the Sargasso Sea, *Carpenter and Price* [1977] reported average *Trichodesmium* concentrations of

1–4 colonies/L in the Caribbean compared to 0.25–0.5 colonies/L in the Sargasso. Thus the range of values predicted by the model over all seasons in these two regions (<0.25 to 4 colonies/L) agrees quite well with the observations. However, the model predicts the highest concentrations in the southern Sargasso Sea, whereas the observations indicate the opposite. This pattern of higher concentrations in the Caribbean reported by *Carpenter and Price* [1977] is also apparent in the data compiled by *Carpenter and Romans* [1991]. This discrepancy may also be related to the fact that the model generates MLDs that are too deep in the Caribbean in winter and spring.

[41] From a compilation of direct rate estimates from numerous cruises in the Caribbean and Sargasso Sea, *Capone et al.* [1997] reported mean N_2-fixation rates ranging from 0.004 to 0.228 mmoles N m^{-2} d^{-1} for Caribbean waters and mean values between 0.001 and 0.006 mmoles N m^{-2} d^{-1} for the Sargasso Sea. However, using some of the same data *Carpenter and Romans* [1991] estimated substantially higher rates (ranging from 0.7 to 3.57 mmoles N m^{-2} d^{-1}) for the same general area. *Orcutt et al.* [2001] estimated maximum summer/fall rates at BATS of 0.01–0.1 mmoles N m^{-2} d^{-1} (depending upon the year in question) for colonies only, with values approaching zero in winter and spring.

[42] For comparison, the model generates integrated rates ranging from about 0.0 to 0.6 mmoles m^{-2} d^{-1} in September in these waters, with the highest values associated with the biomass maximum situated just north of the Greater Antilles, and lower values in the southeastern Caribbean and the Sargasso Sea (Figure 7). During other seasons the model-estimated rates drop to low levels in these waters. In the vicinity of BATS the model predicts low rates throughout the year (<0.06 mmoles m^{-2} d^{-1}). Thus the range of rates generated by the model for the Caribbean and the Sargasso Sea are roughly comparable to those summarized by *Capone et al.* [1997], and they are consistent with the colony-based estimates of *Orcutt et al.* [2001] at BATS. The model-estimated rates are considerably lower than the estimates of *Carpenter and Romans* [1991], but these investigators used very liberal assumptions in their calculations which have been questioned in a subsequent publication [see *Lipschultz and Owens*, 1996].

[43] The seasonal biomass cycle generated by the model in the Sargasso Sea and Caribbean waters is essentially the same as the seasonal cycle in the Gulf of Mexico. *Trichodesmium* biomass begins to increase in April/May following the late winter/early spring phytoplankton bloom in these waters and continues to increase through summer and fall, and then declines in December as the mixed layer deepens and mean light levels drop. This seasonal cycle is similar to that described by *Hood et al.* [2001], and it is driven by the same physical and biological dynamics; that is, *Trichodesmium* growth rates increase and their biomass begins to accumulate after the late winter/early spring phytoplankton bloom declines due to DIN depletion. The combination of relatively shallow mixed layers in the late spring/early summer, high mixed layer light levels, and low DIN concentrations provide optimal conditions for *Trichodesmium* growth, while simultaneously inhibiting phytoplankton growth. As the summer progresses, increasing surface light intensities and surface heating maintain these optimal conditions for *Trichodesmium*. However, due to its slow growth rate, *Trichodesmium* biomass accumulates slowly, with maximum concentrations developing in October and November. Lower mean light levels and surface cooling in December results in deepening of the mixed layer, thereby shutting down *Trichodesmium* growth and mixing the accumulated *Trichodesmium* biomass downward, while simultaneously entraining DIN from depth. The latter sets the stage for the winter/spring phytoplankton bloom and a repeat of the seasonal cycle.

[44] Figure 6 shows that this seasonal cycle in *Trichodesmium* concentration is strongly manifested in the model solution throughout the southwestern North Atlantic. As discussed by *Hood et al.* [2001], *Orcutt et al.*'s [2001] 3-year time series (1995–1997) of *Trichodesmium* biomass and N_2-fixation rate measurements from BATS reveals a seasonal cycle that is very similar to the model-predicted cycle. As discussed above, there is some evidence of this seasonality in the Gulf of Mexico as well. Similarly, high concentrations of *Trichodesmium* are most commonly observed in the southern Sargasso Sea in summer and fall [*Carpenter and Romans*, 1991; *Carpenter et al.*, 2004, and references therein]. Farther south, the populations are more sustained over the seasons, but the seasonal dynamic of the winter trade winds does affect the distribution and growth of *Trichodesmium*. Even in the tropics proper, we expect peak growth and abundance during calm periods in the summer and fall (D. G. Capone, personal observations, 2002). Thus the model-predicted seasonal cycle appears to be consistent with observed patterns in the Sargasso Sea, the Gulf of Mexico, and the Caribbean Sea.

[45] These general observations are supported by a 25-month time series collected by *Navarro* [1998] just south of Puerto Rico, which reveals a clear *Trichodesmium* abundance maximum in July–October 1996 (0.014–0.5 colonies/L) and a weaker maximum in October–November of 1997 (0.003–0.03 colonies/L). However, these data revealed no seasonal maximum in 1995. Moreover, *Carpenter et al.* [2004] report higher concentrations east of Puerto Rico in spring (5–25 colonies/L in May/June 1994) than in fall (0.5–3.0 colonies/L in October/November 1996). Thus there appears to be considerable interannual variability, and it is clear that *Trichodesmium* blooms sometimes develop in these waters in the spring, which is not consistent with the model.

[46] Farther south, time series published by *Steven and Glombitza* [1972] and *Borstad* [1982] for a location about 9 km east of Barbados (13°15′N, 59°43′W), reveals strong oscillations in *Trichodesmium* concentrations with a period of about 3 months, but no evidence of the model-predicted seasonality. Rather, the variability in these waters appears to be dominated by the complex movements of the Guiana Current and the passage of Brazil Current eddies which pass through this region with a period of about 3 months [*Carton and Chao*, 1999]. Since the relatively low resolution of our model does not permit accurate formation and propagation of these eddies, we do not expect to see 3-month fluctuations in *Trichodesmium* biomass in the vicinity of Barbados as observed.

3.2.4. Eastern and Northeastern Coast of Brazil and Offshore Waters in the Vicinity

[47] *Carpenter et al.* [2004] report high concentrations (up to 8 colonies/L) in March–April of 1996 in two

offshore patches off of the northeastern coast of Brazil (one centered at 14°N, 55°W, and another between 30°W and 45°W and 0° and 8°N, Table 1, Figure 5). Although the model does not produce high concentrations in the northern region (14°N, 55°W), it does produce a well-defined *Trichodesmium* population maximum in the southern region (30°–45°W and 0°–8°N) (Figure 6) that is part of a distinct band of high *Trichodesmium* concentration that extends westward along the equator between 0° and 5°N. These model results suggest that the southern patch reported by *Carpenter et al.* [2004] may have been derived from offshore blooms that develop along the flanks of the equatorial upwelling region, which are then advected westward. Note, however, that the predicted concentrations are much lower than observed (<1 colony/L).

[48] *Goering et al.* [1966] reported both *Trichodesmium* biomass and rate measurements from two cruises in the region 0°–24°N, 45°–66°W (off of the northeastern coast of Brazil with most stations located in or near the Amazon River plume). Their *Trichodesmium* biomass measurements suggest concentrations of 1–10 colonies/L with generally higher values in fall [see also *Calef and Grice*, 1966], and they report a mean N_2-fixation rate of about 0.01 mmoles N m^{-3} d^{-1} in fall and values near zero in spring. For comparison, the model predicts low *Trichodesmium* biomass and rates all along the northeastern coast of Brazil in spring (March) and distinctly elevated biomass and rates in summer and fall, with colony concentrations approaching 3 colonies/L and N_2-fixation up to 0.02 mmoles N m^{-3} d^{-1} in June and September, respectively (Figures 6 and 7). Thus the model predicts *Trichodesmium* concentrations and N_2-fixation rates in this region in summer and fall that are largely consistent with the observations, but it may underestimate values in spring.

[49] We know of only one data set from the Brazil coastal region between 5°S and 15°S. On a transect extending through the equator and along the east coast of South America in September–October, *Tyrrell et al.* [2003] observed significant *Trichodesmium* concentrations (0.1–10 colonies/L) on the equator and south along the South American coast between 25°S and 35°S, but they did not observe *Trichodesmium* between 5°S and 15°S. This pattern is consistent with the model, which generates low concentrations (<0.25 colonies/L) off of the east coast of Brazil and higher concentrations in equatorial waters to the north (>0.50 colonies/L) in fall (Figure 6). We have no data to either confirm or refute the relatively high model-predicted *Trichodesmium* concentrations off the east coast of Brazil during other seasons (Figure 6).

[50] Finally, it should be noted that many of the locations discussed in this section are strongly influenced by freshwater inputs from the Amazon and Orinoco Rivers. We know from direct observations that *Trichodesmium* does not occur in low-salinity waters and is therefore absent in many places along the northeast coast of South America where one might otherwise expect it to occur (D. G. Capone and A. Subramaniam, unpublished observations, 2004). Although the freshwater input from these rivers is included in the physical model, our biological model has no mechanism that would prevent *Trichodesmium* from growing in low-salinity waters. In fact, in the model, stratification associated with freshwater input should tend to enhance *Trichodesmium* growth in regions where DIN is depleted. This may result in overestimation of *Trichodesmium* concentrations during periods when the river flow is high and coastal salinities are low (i.e., summer). This fact may help to explain some of the discrepancies discussed above.

3.2.5. Cape Verde/Sierra Leone Region and Equatorial Waters

[51] There are several reports of *Trichodesmium* in tropical waters off of the coast of northwest Africa. For example, *Vallespinos* [1985] reported *Trichodesmium* between 6°N and 24°N from a cruise in November 1975 off of northwest Africa and compared them to measurements in the same general region in August 1971 by *Margalef* [1973]. In both studies, *Trichodesmium* was found in the upwelling region within 2° of the coast and extended offshore to at least 22°W, but the populations were actually associated with warm, nutrient-poor surface waters, derived from the south. The *Trichodesmium* concentrations were an order of magnitude higher in August (1971) compared to November (1975) (Table 1). Vallespinos concluded that standing crop fluctuates seasonally, being most abundant from August to November and absent during spring.

[52] These observations and conclusions are basically consistent with the model results for this region which show the highest concentrations and areal extent in the summer and fall and lowest concentrations and areal extent in the winter and spring (Figure 6). In the model, high *Trichodesmium* concentrations are also associated with nutrient-poor surface waters which are located adjacent to (south of) the upwelling center. However, *Hernańdez-León et al.* [1999] reported *Trichodesmium* much farther offshore (between 30°W and 45°W) and farther north on a zonal (east-west) transect along 22°N in August–September. *Trichodesmium* blooms do not develop this far north or offshore in this region of the North Atlantic in the model. Again, we speculate that this discrepancy may be related to the fact that the model predicts MLDs that are much too deep in the winter months in this region of the North Atlantic which would tend to reduce the northward and seaward extent of *Trichodesmium* populations all year round.

[53] *Tyrrell et al.* [2003] report highly variable (0–10 colonies/L) *Trichodesmium* concentrations in September–October near the Canary Islands (20°N–30°N, 20°W), and high concentrations (1–10 colonies/L) in essentially the same areas where the model produces high concentrations in the Guinea Dome/Sierra Leone region (Figure 6). Their data also reveal generally high concentrations from 0° to 15°N, and 10°W to 25°W, with a patch in excess of 10 colonies/L just north of the equator. In Tyrrell et al.'s data set, *Trichodesmium* concentrations drop dramatically on the equator itself. These recent observations are consistent with earlier reports by *Aleem* [1980], which revealed *Trichodesmium* in Sierra Leone coastal waters, and *Bauerfeind* [1987], who reported the presence of *Trichodesmium* (up to 8.5 colonies/L) between 3°N and 2°S at 22°W in April through June of 1979.

[54] For comparison, the model generates maximum concentrations of 2–5 colonies/L in the Guinea Dome/Sierra Leone region in the fall, up to 9 colonies/L in summer, and between 1 and 4 colonies/L all year round just north of the equator at 10°W (Figure 6). The model also

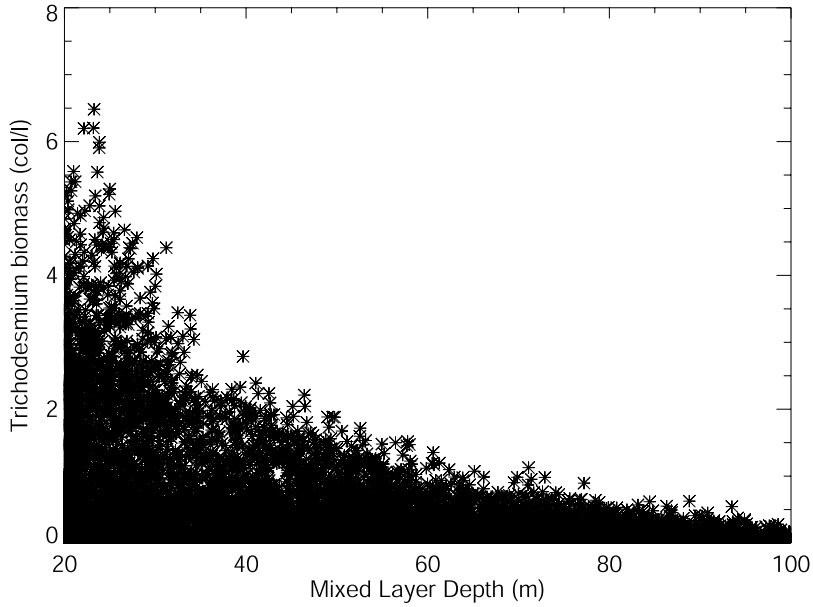

Figure 8. Modeled-estimated *Trichodesmium* concentration in the mixed layer versus modeled-estimated mixed layer depth (MLD) between 20 m (MICOM's minimum MLD) and 100 m.

predicts distinctly lower concentrations in a zonal band between the equator and 5°S all year round, which is consistent with *Tyrrell et al.*'s [2003] fall measurements. Thus the patterns generated by the model in the Guinea Dome/Sierra Leone region and in equatorial waters to the south generally agree with the direct observations, albeit with somewhat lower concentration ranges.

3.2.6. Gulf of Guinea and the South African Coast

[55] The model predicts higher *Trichodesmium* concentrations and rates of N_2-fixation in the Gulf of Guinea in spring than anywhere else in the domain (>9 colonies/L, $\gg$0.02 mmoles N m^{-3} d^{-1}), and according to the model the populations persist there all year round at fairly high levels (>2 colonies/L) (Figures 6 and 7). *Dandonneau* [1971] reported that *Trichodesmium* is present all year in shelf waters in the vicinity of Abidjan (the western reaches of the Gulf of Guinea, 2°W–8°W), and that it is associated with the presence of oligotrophic, oceanic water masses. In addition, the harpacticoid copepod *Macrosetella gracilis*, whose nutrition and life cycle are closely associated with *Trichodesmium* spp. [*O'Neil et al.*, 1996; *O'Neil*, 1997], has also been found, along with *Trichodesmium*, in the same general area (M. Pagano via R. Foster, personal communication, 2002). According to the model the highest *Trichodesmium* concentrations and N_2-fixation rates actually develop farther east (0°E–10°E, 5°N–5°S). As discussed above, the model generates relatively thin MLDs and high average light levels throughout the year in these waters, as observed. The thin mixed layers in this region are due, at least in part, to high freshwater fluxes from direct precipitation and river runoff. Thus it appears that the physical conditions which give rise to the high *Trichodesmium* concentrations in the model actually exist in the Gulf of Guinea. However, the model may underestimate the strength of coastal upwelling in this region, which might lead to overestimation of *Trichodesmium* biomass and N_2-fixation.

[56] Farther south, *An* [1971] reported that *Trichodesmium* was "relatively common" along two meridional transects (11°S and 14°S) extending offshore from southern Africa (Angola) in April of 1968. In contrast, *Tyrrell et al.*'s. [2003] southeastern transect (which ran from off the coast of Sierra Leone diagonally down to the South African coast at 20°S, in September–October) shows *Trichodesmium* (0.1–1 colonies/L) at only one station just south of the equator. No *Trichodesmium* was encountered farther south and east in the vicinity of An's transects. This difference probably reflects seasonal variations in the populations; that is, *Trichodesmium* is present in Austral fall and absent in Austral spring. The model results are consistent with both of these reports (Figure 6), predicting lower concentrations south of the equator in Austral Spring (September) as reported by Tyrrell, and elevated concentrations south of the equator in Austral fall (March) as observed by An, with concentrations ranging from 0.25 to 1 colonies/L.

3.2.7. Relation Between MLD and N_2-Fixation

[57] Figure 8 shows that the highest *Trichodesmium* biomass in the model occurs when the MLD is at or near the minimum thickness (i.e., <30 m) and the biomass gets progressively lower as MLD increases. This plot, however, also reveals that colony concentrations are often low when the mixed layer is thin and sometimes fairly high when the mixed layer is relatively thick. This lack of a tight correlation between MLD and biomass arises because (1) time is an important factor in determining whether or not high biomass develops; that is, the mixed layer must remain relatively thin long enough to allow significant *Trichodesmium* concentrations to accumulate; and (2) thin mixed layers that develop in response to upwelling can have high phytoplankton concentrations that lower light levels and prevent *Trichodesmium* growth. Conversely, relatively thick mixed layers (i.e., approaching 60 m, Figure 8) can give rise to high colony concentrations if they persist and become DIN depleted so that phytoplankton concentrations remain low and there is

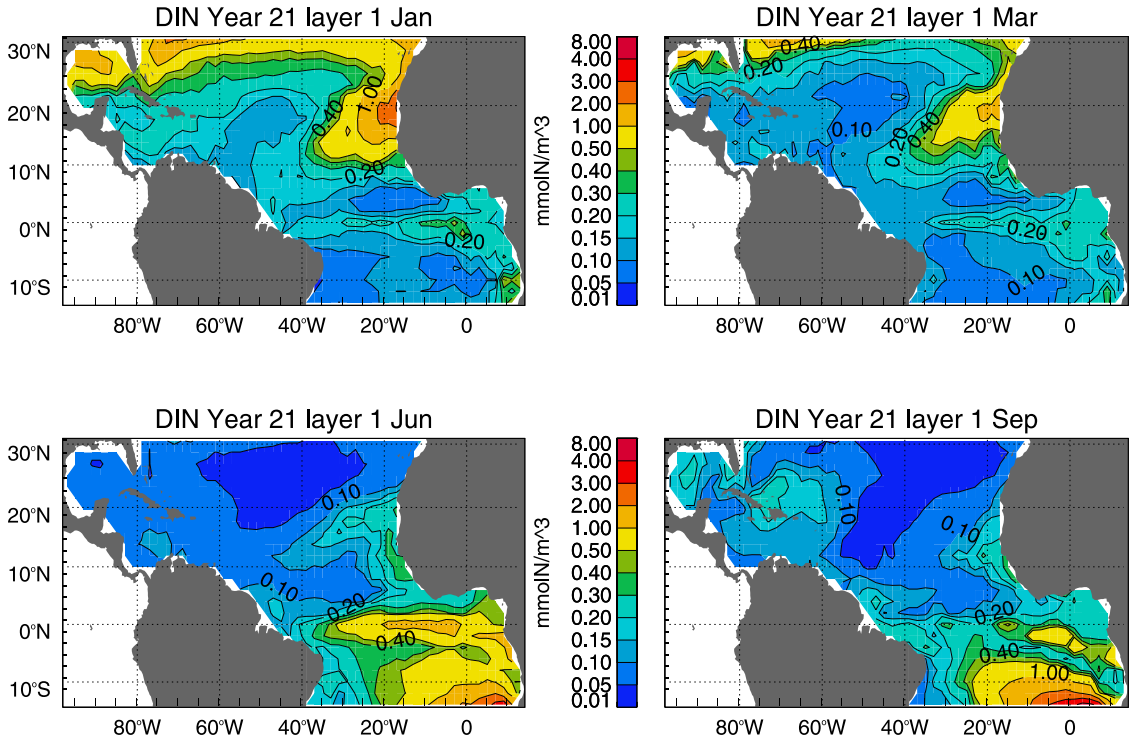

Figure 9. Model-estimated DIN concentrations in the mixed layer. The fields are synoptic, from the middle of the specified month. The concentration units are mmoles N m^{-3}.

time to allow a significant *Trichodesmium* biomass to develop. Deep mixed layers can also contain elevated colony concentrations when high surface accumulations are mixed downward by a mixing event. Thus the model is capable of generating elevated *Trichodesmium* concentrations under windy/deep MLD conditions, which has been recently observed in the field (A. Subramaniam, personal communication, 2003).

3.3. Modeled and Observed DIN Concentrations

[58] The temporal and spatial patterns in mixed layer DIN concentrations generated by the model primarily reflect patterns in the physical processes which bring nutrients into surface waters (Figure 9); for example, DIN concentrations are enhanced in upwelling regions off of northwest Africa and along the equator. In addition, concentrations are substantially elevated in winter (January) prior to the spring phytoplankton bloom north of 20°N and in the Gulf of Mexico due to deep winter mixing. DIN concentrations are similarly elevated in the austral winter (June and September) south of 10°S.

[59] However, not all of the regions of enhanced DIN concentration in the model can be attributed to physical processes. Elevated concentrations (up to 0.4 mmoles N/m^3) are also apparent in the Gulf of Mexico, the southern Sargasso Sea and generally throughout much of the southwestern North Atlantic in late summer and fall (September). A comparison between Figures 6, 7, and 9 shows that these regions of enhanced DIN concentration are coincident with regions of high *Trichodesmium* concentration and high rates of N_2-fixation. Although the effects are more subtle, DIN concentrations are also significantly enhanced by N_2-fixation off the coast of Africa where the model-estimated N_2-fixation rates are high (i.e., in the Gulf of Guinea, and coastal Africa up into the Cape Verde/Sierra Leone region).

[60] Figures 10 and 11 show sections of DIN concentration from the model (bottom panels) and from the NODC analyzed [*Conkright et al.*, 1998] seasonal climatologies (top panels) along two meridional sections, one extending north from the coast of South America up through the Caribbean and the Sargasso Sea along 70°W (Figure 10), and another extending north through the equator and up along the coast of northwest Africa along 21°W (Figure 11). The 70°W sections show that the model generates the same broad patterns in the nutrient distributions as observed, with the nutricline extending up nearer to the surface at the northern and southern extremes of the transect, and generally lower values at depth in the vicinity of 20°N.

[61] The climatology also shows two distinct near-surface DIN maxima along the 70°W transect. One of these is centered at about 15°N in the middle of the Caribbean Sea, and it persists throughout the year. This feature, which is not represented in the model, has DIN concentrations which vary from 0.4 to >1.0 mmoles N/m^3, and concentrations are highest in June and September. The second near-surface DIN anomaly is located between 20°N and 25°N, and appears only in June and September. This latter feature, which has concentrations in excess of 0.4 mmoles/m^3 in September, does appear to be crudely represented in the model as a broad region of elevated DIN concentrations between 19°N and 25°N. In the model this anomaly is generated by *Trichodesmium* and N_2-fixation, as discussed above. We speculate that the persistent near-surface DIN anomaly that is observed in the Caribbean Sea at about

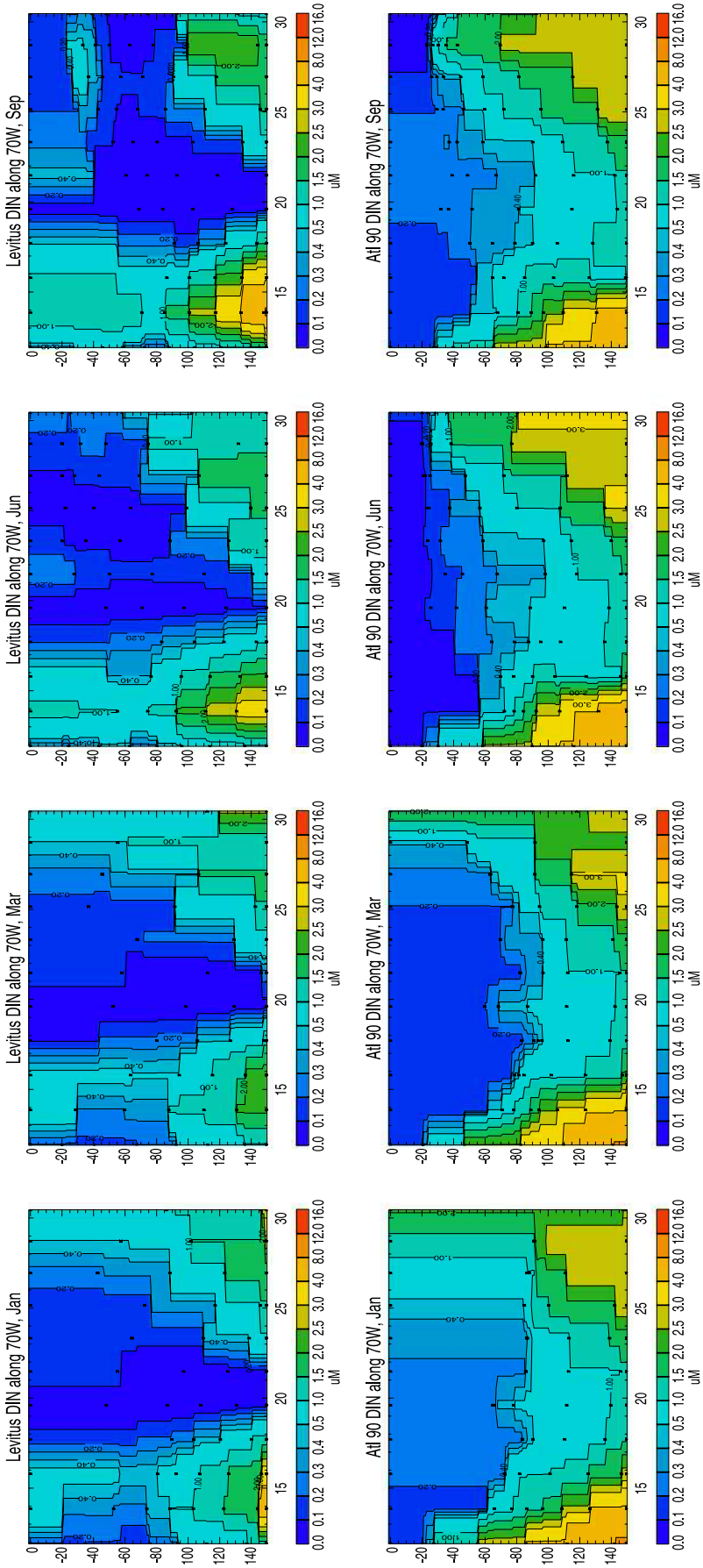

Figure 10. Model-estimated (bottom row) and observed, climatological (top row) DIN concentrations along 70°W down to 150 m depth. The section extends from the northern coast of South America up through the Caribbean and Sargasso Seas to 32°N. The model fields are synoptic, from the middle of the specified month, and the observed fields are seasonal climatologies from the NODC Analyzed fields from the World Ocean Database 1998 CD-ROM set [*Conkright et al.*, 1998] which have been interpolated onto the modeled levels.

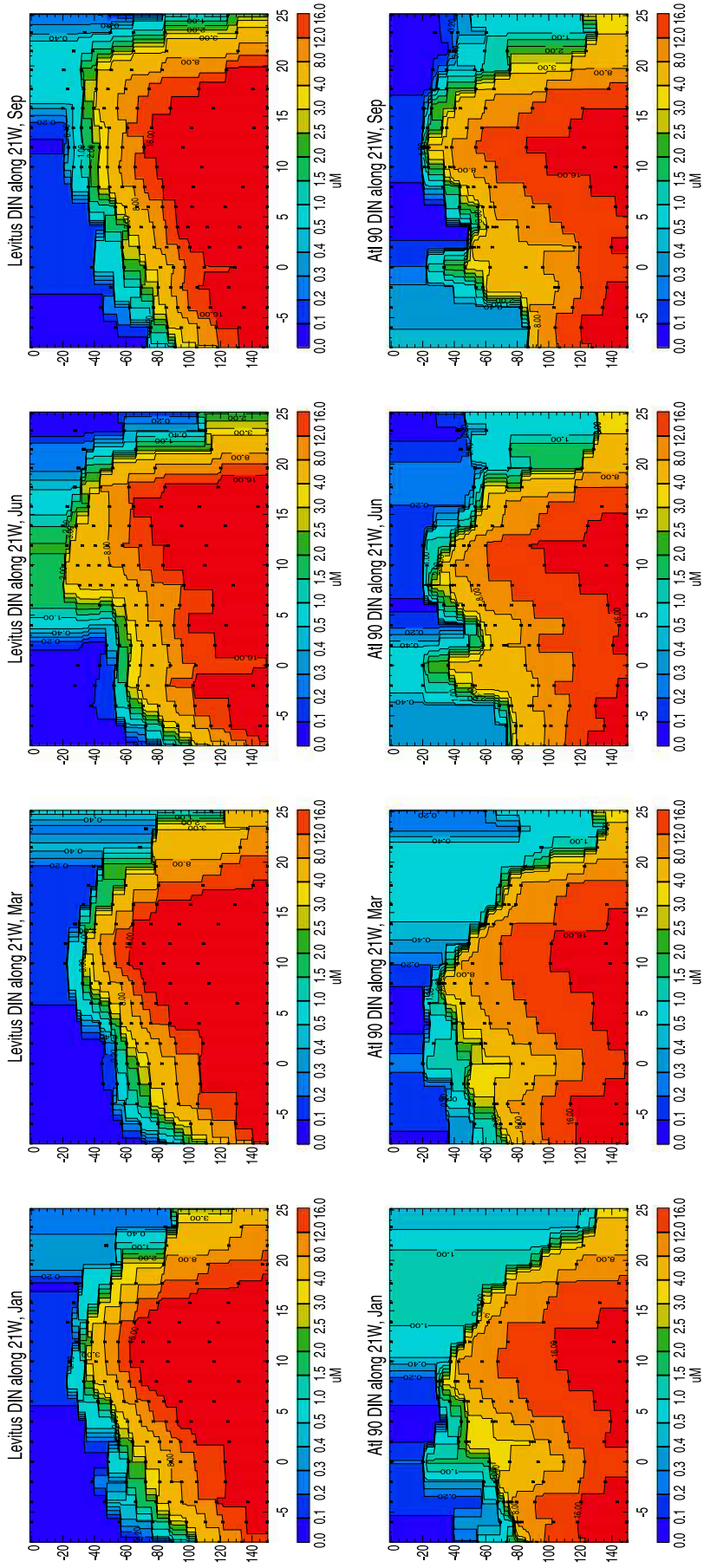

Figure 11. As in Figure 10 along 21°W extending from 8°S to 25°N.

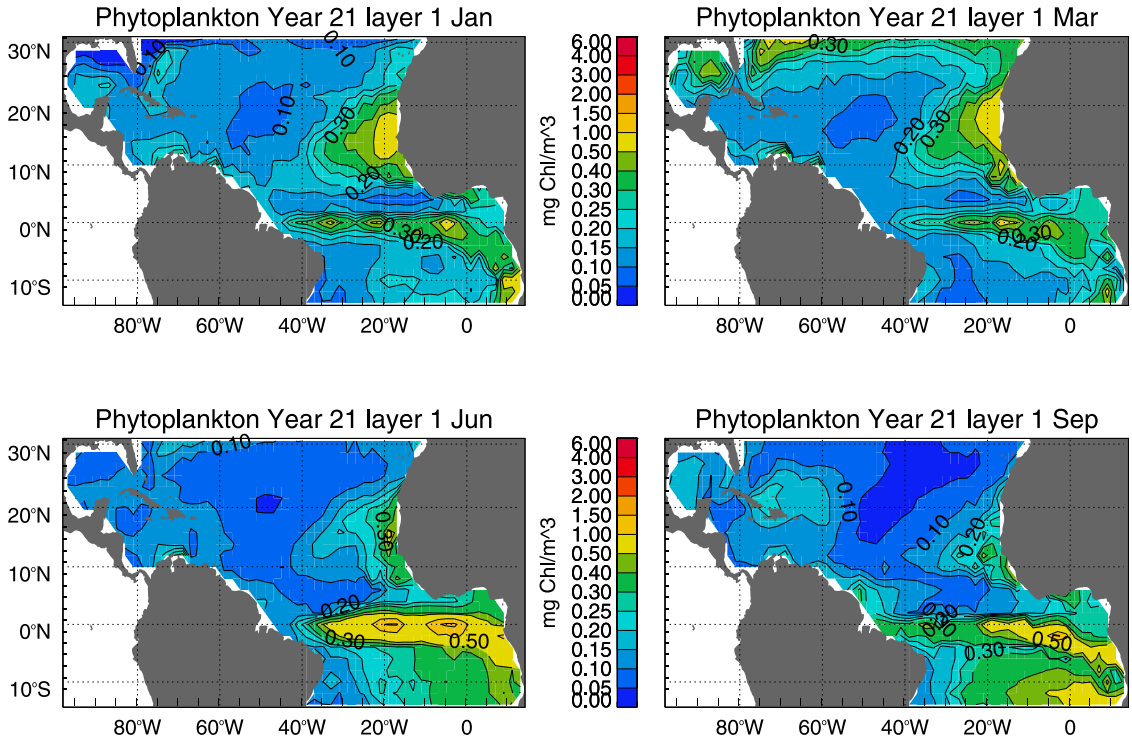

Figure 12. Modeled-estimated phytoplankton concentration in the mixed layer. The fields are synoptic, from the middle of the specified month. Concentrations are expressed in mg Chla/m^3. Chlorophyll concentration was estimated from the model units (mmoles N/m^3) assuming a C:N ratio of 106:16 (mole:mole) and a C:chla ratio of 50:1 (wt:wt).

15°N may also be generated by N_2-fixation, but does not show up in the model because the model underestimates *Trichodesmium* and N_2-fixation in these waters.

[62] A comparison between the model and observed DIN concentrations along 21°W (Figure 11) shows that the model reproduces the large-scale meridional patterns on the eastern side of the basin as well, i.e., with the nutricline depth gradually shoaling from 10°S to 10°N and then deepening rapidly at the northern end of the transect. The effects of equatorial upwelling are much more obvious in the model solution than they are in the observations. This difference between the model and the observations is probably due, in part, to the overly strong equatorial upwelling in the model, as discussed above, and in part to the smearing of the equatorial upwelling signal in the observations due to averaging and interpolation of the data. Note also that the nutricline is not as sharp in the model as observed. The fact that this discrepancy exists, even though the pycnocline structure in the model is as sharp as observed (not shown), suggests that remineralization of particulate matter may be occurring too slowly (deeply) in the model. Effects of *Trichodesmium* and N_2-fixation are not obvious along this section in the model, but they do influence the near-surface DIN concentrations [*Coles et al.*, 2004a].

3.4. Modeled and Observed Phytoplankton Concentrations

[63] The model reproduces the gross large-scale patterns and temporal variations in phytoplankton chlorophyll concentrations that are observed in SeaWiFS imagery (Figures 12 and 13). However, the model has a general tendency to underestimate coastal chlorophyll concentrations. Some of these discrepancies are probably due to the effects of nutrient inputs from rivers that are not represented in the model (e.g., in the vicinities of the Amazon and Orinoco River outflow plumes), and/or these turbid and DOM-rich plumes may cause SeaWiFS to overestimate chlorophyll concentrations [*O'Reilly et al.*, 1998]. Off the coast of northwest Africa, a more likely explanation is that the model cannot properly represent the intense coastal upwelling very near shore due to its relatively low horizontal resolution. In contrast, the model consistently overestimates chlorophyll concentrations along the equator because the upwelling in the physical model is too vigorous and extends too far to the west along the equator (see discussion in section 3.1).

[64] Of course, the overall chlorophyll concentrations (and levels of primary productivity) generated by the model are a matter of choice; that is, we tuned chlorophyll concentrations in the mixed layer to roughly approximate the SeaWiFS observed values by adjusting export levels in the model. The general tendency of the model to underestimate chlorophyll concentration in some regions arises because the model had to be "tuned down" somewhat to avoid generating extremely high chlorophyll concentrations at the equator and adjacent waters. These kinds of discrepancies between modeled and observed physical fields and surface chlorophyll concentrations are commonly observed with low-resolution 3-dimensional biogeochemical models, and they have been discussed extensively in the literature [see *Oschlies and Garcon*, 1999; *Oschlies*, 2000, and references therein].

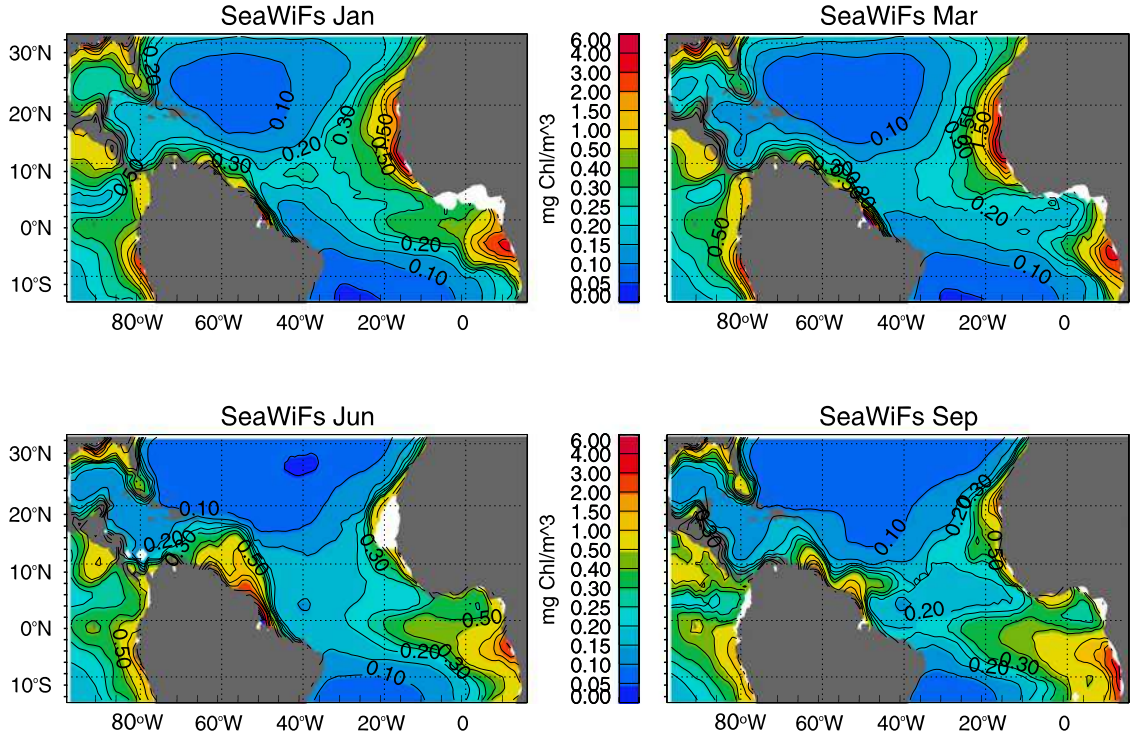

Figure 13. Monthly climatological near-surface chlorophyll concentration from SeaWiFS in mg Chla/m^3. The climatologies are simple averages of all available data for each month, collected from September 1997 through July 2001.

[65] The effects of new nitrogen inputs from N_2-fixation on the model-generated chlorophyll concentrations can be see quite clearly in the southwestern North Atlantic in the fall (September) (compare Figures 6, 7, 9, and 12). Note in particular the distinctly elevated phytoplankton concentrations in the model solution in four regions: (1) around Cuba and Haiti extending northeastward into the open ocean; (2) off the northern coast of South America and in the Caribbean Sea; (3) along the western side of the Gulf of Mexico; and (4) off of the southwestern tip of Florida. Although more subtle, N_2-fixation also enhances the model-generated phytoplankton concentrations off the coast of northwest Africa in the Cape Verde/Sierra Leone region, in the Gulf of Guinea, and in two broad zonal bands situated to the north and south of the equator. These effects are discussed in more detail in section 3.5 below.

[66] It is difficult to discern from these SeaWiFS surface chlorophyll maps (Figure 13) whether or not this enhancement of surface phytoplankton concentrations by N_2-fixation actually occurs in nature. Figure 13 does not reveal any obvious enhancement of chlorophyll concentrations in the southern Sargasso Sea in the fall, as predicted by the model, even though the observed DIN sections suggest that there may actually be some enhancement of nutrient concentrations due to N_2-fixation (i.e., observed elevated surface DIN concentrations in June and September between 20°N and 25°N in Figure 10, top panels). However, a recent EOF analysis of the SeaWiFS chlorophyll data has revealed a summertime anomaly (enhancement) of chlorophyll concentrations around Cuba and Haiti as predicted by the model [*Coles et al.*, 2004b]. On the eastern side of the Atlantic basin, all we can say for certain about the effects of N_2-fixation is that the modeled chlorophyll concentrations are too low compared to SeaWiFS in the Gulf of Guinea in model runs without input of new nitrogen from N_2-fixation [see *Coles et al.*, 2004a].

[67] This general sequence of events, where new nitrogen inputs from *Trichodesmium* blooms give rise to subsequent increases in other phytoplankton species, has been observed and discussed previously. For example, *Burford et al.* [1995] argue that *Trichodesmium* enhances the growth of other algae. *Devassy et al.* [1979] provide a particularly good example of phytoplankton succession following a *Trichodesmium* bloom, suggesting that nutrient inputs and "conditioning" provided by *Trichodesmium* promotes the growth of diatoms, specifically that of *Nitzschia colosterium* [*Devassy*, 1987]. In contrast, *Revelante et al.* [1982] discuss specific floristic groups associated with *Trichodesmium* and allude to marked increases in dinoflagellates following *Trichodesmium* blooms.

[68] Recent work in the Gulf of Mexico suggests that inputs of new nitrogen from *Trichodesmium* and N_2-fixation may be responsible for initiating harmful algal blooms [*Lenes et al.*, 2001; *Walsh and Steidinger*, 2001; J. J. Walsh, personal communication, 2000]. Specifically, Walsh and Steidinger hypothesize that N_2-fixation supplies the excess nitrogen that is required to support *Karenia brevis* (formerly known as *Gymnodinium breve*) blooms. Although our model does not include specific phytoplankton groups, the enhancement of phytoplankton concentrations due to new nitrogen inputs from N_2-fixation in the model is essentially the same kind of effect; that is, N_2-fixation supplies new nitrogen which stimulates phytoplankton growth. In the model this stimulation of phytoplankton growth happens

only under stratified conditions that are conducive to *Trichodesmium* growth. These are exactly the kind of conditions under which flagellate and dinoflagellate blooms occur. Perhaps it is only a coincidence, but Figure 12 shows that the model predicts a N_2-fixation induced "bloom" off of the southwestern tip of Florida in the fall in the same general area where *K. brevis* blooms occur, and in the western Gulf as well.

3.5. Meridional Sections

[69] The seasonality in *Trichodesmium* concentrations discussed above can be seen very clearly along 70°W (Figure 14), i.e., low concentrations in winter/spring (January and March) and highest concentrations in fall (September). Note that the increased *Trichodesmium* concentrations in June (at about 20°N, just north of Haiti and the Dominican Republic) are located in waters with relatively low DIN (Figure 9) and phytoplankton concentrations. By September the *Trichodesmium* biomass has increased to more than 4 col/L, and the phytoplankton, DIN (Figure 9) and DON concentrations have increased in the mixed layer as well due to new nitrogen inputs from N_2-fixation, as discussed above.

[70] Figure 14 also shows that the vertical distribution of *Trichodesmium* and phytoplankton along this transect is consistent with direct observations from these same waters [*Hood et al.*, 2001; *Carpenter et al.*, 2004], and our general understanding of the relationship between *Trichodesmium* and phytoplankton distributions; that is, *Trichodesmium* populations tend to be restricted to the upper 50 m of the water column where light levels are high and DIN concentrations are low [*Capone et al.*, 1997]. In some sections we also see the development of subsurface phytoplankton maxima at the base of the mixed layer and the top of the nutricline, just below *Trichodesmium*. As discussed by *Hood et al.* [2001], this happens in the model because *Trichodesmium* growth is maximized near the surface where irradiance is highest, whereas phytoplankton growth tends to be constrained by the availability of DIN supplied from depth.

[71] The section along 21°W reveals a more complicated pattern (Figure 15). One can discern three distinct *Trichodesmium* biomass maxima in March and June: one on either side of the equatorial upwelling region and a third off of northwest Africa in the Cape Verde/Sierra Leone region. In January and September, only two of the three maxima are apparent, with the southernmost feature absent. In addition, the *Trichodesmium* maximum off of northwest Africa is much more pronounced in summer and fall (June and September) than it is in winter and spring (January and March).

[72] A comparison of the *Trichodesmium*, phytoplankton, and DIN sections (Figures 11 and 15) reveals that these regions of elevated *Trichodesmium* are located adjacent to regions where the phytoplankton biomass and DIN concentrations are highest. Thus the patterns differ somewhat from what we observe along 70°W where all of the maxima coincide. For example, in June the two *Trichodesmium* concentration maxima on either side of the equator are situated just north and south of the phytoplankton and DIN maxima generated by equatorial upwelling. A similar pattern can be seen off of northwest Africa in June where the highest *Trichodesmium* concentrations are located just south of the highest phytoplankton and DIN concentrations. It should be emphasized, however, that there is also considerable overlap in these distributions, with *Trichodesmium* generally increasing as phytoplankton and DIN concentrations decline. Also note that the model generates distinct subsurface phytoplankton biomass maxima in all seasons, and that the regions of high *Trichodesmium* are always located above these subsurface features.

[73] The DON sections in Figure 15 also reveal distinct maxima. Some of these appear to be associated with elevated phytoplankton biomass and are likely generated by recycling of organic nitrogen derived from new nitrogen (DIN) inputs from upwelling. However, others (e.g., the DON maxima in the mixed layer in June and September between 10°N and 15°N) are clearly associated with elevated *Trichodesmium* concentrations and are likely generated by direct DON exudation from *Trichodesmium*. The latter is consistent with the interpretation of *Vidal et al.* [1999], who argue that elevated DON off of northwest Africa is derived from N_2-fixation.

[74] These model results are consistent with our current understanding of phytoplankton species succession in these waters [*Margalef*, 1963a, 1963b]. Margalef proposed that *Trichodesmium* populations increase along the periphery of upwelling regions in a time/space successional sequence after bloom forming species, such as chain-forming diatoms, have depleted surface nutrient concentrations from recently upwelled waters. We interpret the patterns along 21°W as a manifestation of this successional sequence; that is, we see an upwelling-induced phytoplankton bloom at the equator and off of northwest Africa in all of the sections. This bloom happens because the upwelling brings DIN to the surface and injects it into a thin mixed layer (high mean light). As this water moves laterally away from the upwelling center, the phytoplankton concentrations drop because they deplete the surface DIN concentrations and their growth becomes nutrient-limited. This, in turn, provides an opportunity for *Trichodesmium* populations to increase along the flanks of the upwelling region where the mixed layer is still thin (high light), and DIN and phytoplankton concentrations are lower. However, as the mixed layer gets progressively thicker as water moves laterally away from the upwelling region, the growth rate and biomass of *Trichodesmium* ultimately declines due to light limitation.

4. Summary and Conclusions

[75] In this paper we have attempted to model the distribution of *Trichodesmium* and rates of N_2-fixation in the Atlantic using a coupled physical-biological model, and validate these results using available observations. Following *Hood et al.* [2001], we have hypothesized that *Trichodesmium*'s fundamental physical, chemical, and ecological niche is defined by high light intensity, relatively weak vertical mixing, and low DIN concentrations, where the latter prevents the growth of other, faster growing, phytoplankton species. Further, we have assumed that there is no temperature control of *Trichodesmium* growth rate in our model and that Fe and P limitation do not dictate when or where *Trichodesmium* occurs.

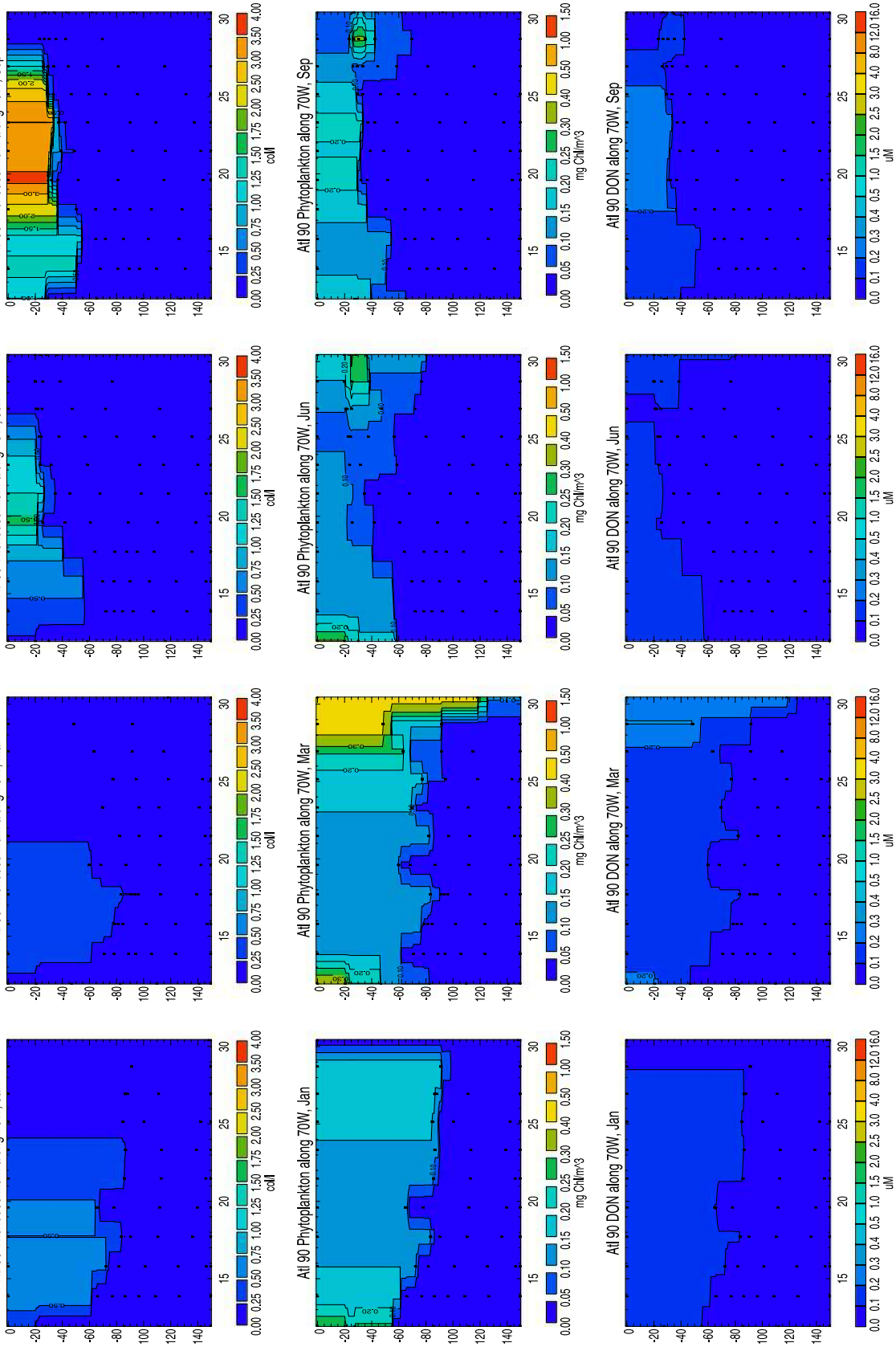

Figure 14. Model-estimated *Trichodesmium*, phytoplankton and DON concentrations along 70°W down to 150 m depth. The section extends from the northern coast of South America up through the Caribbean and Sargasso Seas to 32°N. The model fields are synoptic, from the middle of the specified month. *Trichodesmium* concentration is expressed in colonies/liter, phytoplankton concentration in mg chla/m^3 (following assumptions specified in Figure 11 caption), and DON concentration in μmoles N/L.

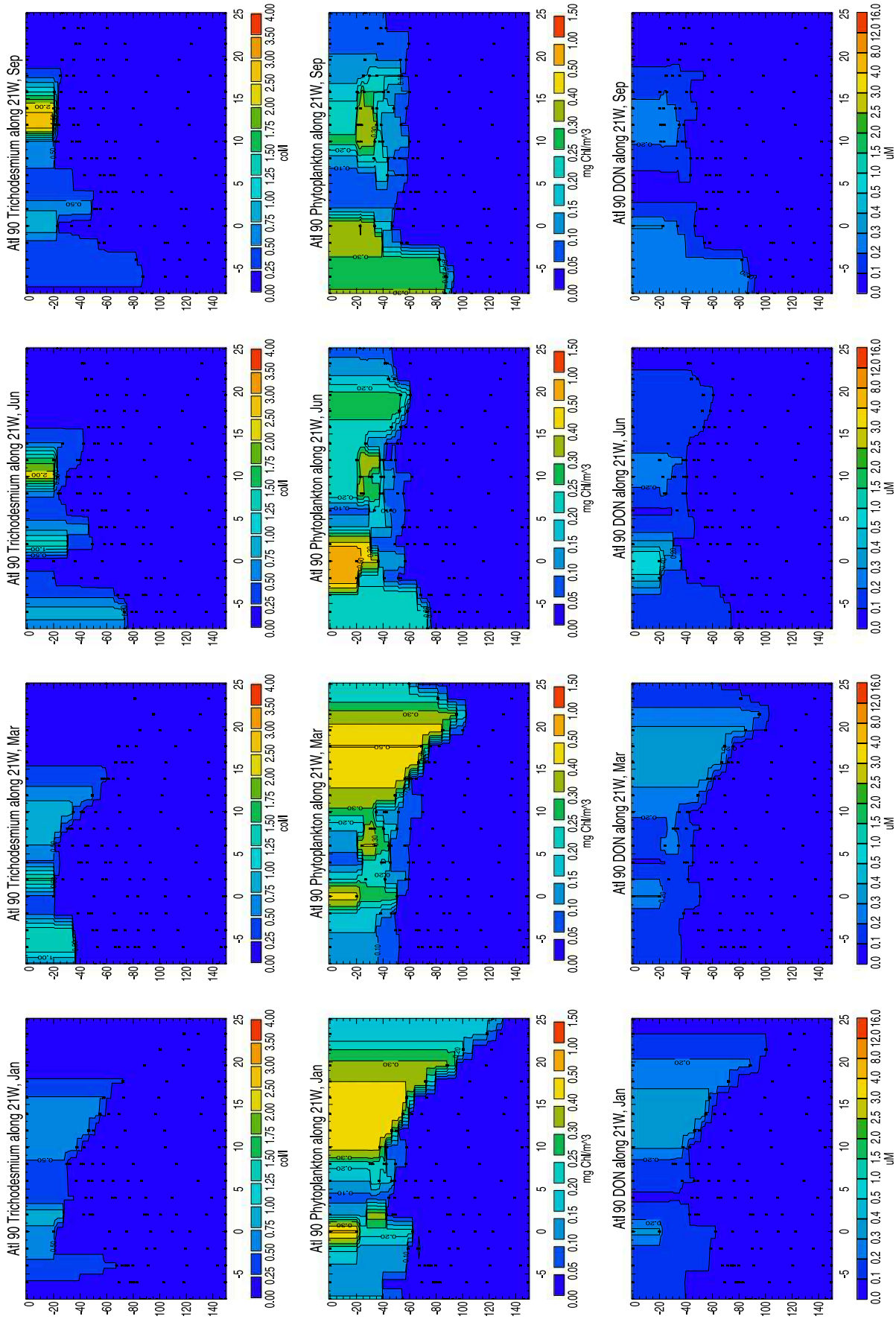

Figure 15. As in Figure 14 along 21°W extending from 8°S to 25°N.

[76] In spite of these simplifying assumptions, the model appears to reproduce the observed large-scale (meridional), *Trichodesmium* distribution pattern in the Atlantic; that is, *Trichodesmium* occurs only in subtropical and tropical waters and concentrations are highest in the latter [*Capone et al.*, 1997]. The model does this without invoking any temperature dependence or mechanical influence on *Trichodesmium* growth rate. Rather, it reproduces the observed distribution in response to meridional gradients in MLD and MLD variability.

[77] We have compiled a fairly large number of measurements from the southwestern North Atlantic which show that the model is reproducing major aspects of the observed temporal and spatial variability in *Trichodesmium* populations, i.e., highest concentrations in summer and fall and distinct population maxima in the Gulf of Mexico and the southern Sargasso Sea/Northern Caribbean. However, the model does not generate the extreme high densities that are sometimes observed in these waters, which we attribute to the formation of near-surface accumulations that cannot be reproduced by the model.

[78] Although we have fewer measurements to compare with, it is clear that the model is generating distinctly elevated *Trichodesmium* concentrations in locations where it has been observed off of northwest Africa, Cape Verde/Sierra Leone, and in equatorial waters. There is also some evidence of *Trichodesmium* blooms occurring off of the coast of South Africa as modeled. Perhaps the biggest question raised by the model-predicted *Trichodesmium* distributions is whether or not the high population densities and high rates of N_2-fixation generated by the model in the Gulf of Guinea are correct. If the concentrations and rates in this area are as high and seasonally persistent as the model suggests, then it is likely that this region is a globally significant center of N_2-fixation that needs to be explicitly considered in global N_2-fixation rate estimates.

[79] Our comparisons also reveal some clear discrepancies between the model and direct measurements of *Trichodesmium* concentration. In some cases, these can be linked to infidelities in the physical model's representation of the mixed layer depth or its temporal evolution. For example, although we expect and observe seasonality in *Trichodesmium* populations in Caribbean waters due to seasonal changes in the strength of the trade winds, it appears that the seasonal cycle generated by the model is too strong due to overly deep winter mixing. Another conclusion that can be drawn from these comparisons is that the model has a general tendency to underestimate the observed *Trichodesmium* populations and rates of N_2-fixation. In some locations, for example, in the open ocean off of the northeastern coast of Brazil, the model produces almost no *Trichodesmium* biomass and very low rates in regions where direct measurements clearly show substantial populations and high rates of N_2-fixation.

[80] The temporal and spatial patterns in mixed layer DIN concentrations generated by the model reveal regions of enhanced surface DIN concentrations that can be clearly attributed to inputs of new nitrogen from *Trichodesmium* and N_2-fixation. In particular, elevated concentrations are apparent in the Gulf of Mexico, the southern Sargasso Sea, and throughout much of the southwestern North Atlantic in the fall. Although the effects are more subtle, DIN concentrations are also significantly enhanced by N_2-fixation off the coast of Africa where the model-estimated rates are high. Interestingly, climatological meridional DIN sections in the western Atlantic appear to confirm some of these model predictions.

[81] The effects of new nitrogen inputs from N_2-fixation on the model-generated phytoplankton fields are readily apparent in the Gulf of Mexico, the Caribbean Sea, and the southern Sargasso Sea in the fall. The model-predicted enhancement of chlorophyll concentrations in the southern Sargasso Sea due to N_2-fixation is not readily apparent in the climatological SeaWiFS data presented in this paper (Figure 13). However, a recent EOF analysis of SeaWiFS chlorophyll data has revealed enhancement in this region as predicted by the model [*Coles et al.*, 2004b]. Moreover, there are several publications and accounts from other areas which suggest that new nitrogen inputs from *Trichodesmium* influence phytoplankton concentrations [e.g., *Burford et al.*, 1995; *Devassy et al.*, 1979; *Devassy*, 1987; *Revelante et al.*, 1982; *Lenes et al.*, 2001; *Walsh and Steidinger*, 2001; J. J. Walsh, personal communication, 2000].

[82] Stepping back and looking at the full sequence generated by the model reveals a three-step succession where (1) elevated DIN concentrations stimulate phytoplankton growth, which is followed by (2) *Trichodesmium* growth after DIN depletion, which is then followed by (3) enhanced phytoplankton growth due to new nitrogen inputs from N_2-fixation. Although we do not resolve different phytoplankton species or forms of DIN in our model, we interpret this sequence as representing something like a diatom-*Trichodesmium*-flagellate succession, where upwelling or mixing stimulates a strong diatom bloom in a nitrate-rich environment and *Trichodesmium* stimulates a weaker flagellate bloom in a stratified ammonium, urea, and DON rich environment.

[83] The results presented in this paper lead us to conclude that our model includes the fundamental factors that control spatial and temporal variations in *Trichodesmium* concentrations and rates of N_2-fixation in the Atlantic Ocean. Moreover, it appears that our model also reproduces some of the major effects that these diazotrophically derived inputs of new nitrogen have on the pelagic ecosystem. Thus we do not reject the *Hood et al.* [2001] hypothesis; that is, we believe that *Trichodesmium*'s fundamental physical, chemical, and ecological niche is defined by high light intensity, relatively weak vertical mixing, and low DIN concentrations, where the latter prevents the growth of other, faster growing, phytoplankton species. Further, we conclude that although Fe and P limitation may place constraints upon the total amount of *Trichodesmium* biomass that can develop in any one location, these elements do not dictate when or where *Trichodesmium* occurs.

[84] **Acknowledgments.** We would like to thank Ajit Subramaniam and Edward Carpenter for providing many of the references that were used to validate the modeled-generated *Trichodesmium* distributions, and Mercedes Pascual for helpful discussions on various aspects of this work. We thank Toby Tyrrell for generously allowing us to use his Atlantic transect data to validate our model before his data were published, and Tracy Villareal for assisting with efforts to validate the model in the Gulf of Mexico. We also thank Cara Wilson for generating the SeaWiFS chlorophyll composites shown in Figure 12. This work was supported by an NSF Biocomplexity Initiative grant to R. Hood, V. Coles (OCE-9981218), and D. Capone (OCE-9981371). This paper represents UMCES contribution 3743.

References

Aleem, A. (1980), Marine Cyanophyta from Sierra Leone (West Africa), *Bot. Mar.*, *23*, 49–51.

An, C. N. (1971), Atlantic Ocean phytoplankton south of the Gulf of Guinea on profiles along 11 and 14°S, *Oceanology*, *7*, 896–901.

Bauerfeind, E. (1987), Primary production and phytoplankton biomass in the equatorial region of the Atlantic at 22°W, *Oceanol. Acta*, *10*, 131–136.

Bauerfeind, E., R. Boje, E. Fahrbach, J. Lenz, M. Meyerhofer, and M. Rolke (1983), Planktological and chemical data from the equatorial Atlantic at 22W obtained in February to June 1979, report, Inst. Meereskunde, Kiel.

Berman-Frank, I., J. T. Cullen, Y. Shaked, R. M. Sherrell, and P. G. Falkowski (2001), Iron availability, cellular iron quotas, and nitrogen fixation in *Trichodesmium*, *Limnol. Oceanogr.*, *46*, 1249–1260.

Bleck, R., and L. T. Smith (1990), A wind-driven isopycnic coordinate model of the North and Equatorial Atlantic Ocean: 1. Model development and supporting experiments, *J. Geophys. Res.*, *95*, 3273–3285.

Bleck, R., C. Rooth, D. Hu, and L. T. Smith (1992), Salinity-driven transients in a wind- and thermohaline-forced isopycnic coordinate model of the North Atlantic, *J. Phys. Oceanogr.*, *22*, 1486–1505.

Borstad, G. A. (1982), The influence of the meandering Guiana Current on surface conditions near Barbados—Temporal variations of *Trichodesmium* (Cyanophyta) and other plankton, *J. Mar. Res.*, *40*, 435–452.

Burford, M. A., P. C. Rothlisberg, and Y. Wang (1995), Spatial and temporal distribution of tropical phytoplankton species and biomass in the Gulf of Carpentaria, Australia, *Mar. Ecol. Prog. Ser.*, *118*, 255–266.

Calef, G. W., and G. Grice (1966), Relationship between the blue-green alga *Trichodesmium* thiebautii and the copepod *Macrosetella gracilis* in the plankton off northeastern South America, *Ecology*, *47*, 855–856.

Capone, D. G., J. P. Zehr, H. W. Paerl, B. Bergman, and E. J. Carpenter (1997), *Trichodesmium*, a globally significant marine cyanobacterium, *Science*, *276*, 1221–1229.

Carpenter, E. J. (1983), Physiology and ecology of marine planktonic *Oscillatoria* (*Trichodesmium*), *Mar. Biol. Lett.*, *4*, 69–85.

Carpenter, E. J. and D. G. Capone (1992), Nitrogen fixation in *Trichodesmium* blooms, in *Marine Pelagic Cyanobacteria: Trichodesmium and Other Diazotrophs*, edited by E. J. Carpenter, D. G. Capone, and J. G. Rueter, pp. 211–217, Kluwer Acad., Norwell, Mass.

Carpenter, E. J., and C. Price (1977), Nitrogen fixation, distribution, and production of *Oscillatoria* (*Trichodesmium*) spp. in the western Sargasso and Caribbean Seas, *Limnol. Oceanogr.*, *22*, 60–72.

Carpenter, E. J., and K. Romans (1991), Major role of the cyanobacterium *Trichodesmium* in nutrient cycling in the North Atlantic Ocean, *Science*, *254*, 1356–1358.

Carpenter, E. J., J. M. O'Neil, R. Dawson, D. G. Capone, P. J. A. Siddiqui, T. Roenneberg, and B. Bergman (1993), The tropical diazotrophic phytoplankter *Trichodesmium*: Biological characteristics of two common species, *Mar. Ecol. Prog. Ser.*, *95*, 295–304.

Carpenter, E. J., A. Subramaniam, and D. G. Caponem (2004), Biomass and primary productivity of the cyanobacterium, *Trichodesmium* spp., in the tropical N. Atlantic Ocean, *Deep Sea Res., Part I*, *51*, 173–203.

Carton, J. A. (1991), Effect of seasonal surface fresh-water flux on sea-surface temperature in the tropical Atlantic Ocean, *J. Geophys. Res.*, *96*, 12,593–12,598.

Carton, J. A., and Y. Chao (1999), Caribbean Sea eddies inferred from TOPEX-Poseidon altimetry and a 1/6° Atlantic Ocean model simulation, *J. Geophys. Res.*, *104*, 7743–7752.

Chassignet, E. P., and Z. D. Garraffo (2001), Viscosity parameterization and the Gulf Stream separation, in *From Stirring to Mixing in a Stratified Ocean: Proceedings of the "Aha Hulikoa" Hawaiian Winter Workshop, University of Hawaii, January 15–19, 2001*, edited by P. Muller and O. Henderson, pp. 37–41, Univ. of Hawaii at Manoa, Honolulu.

Coles, V. J., R. R. Hood, M. Pascual, and D. G. Capone (2004a), Modeling the impact of *Trichodesmium* and nitrogen fixation in the Atlantic Ocean, *J. Geophys. Res.*, C06007, doi:10.1029/2002JC001754.

Coles, V. J., C. Wilson, and R. R. Hood (2004b), Remote sensing of new production fueld by nigrogen fixation, *Geophys. Res. Lett.*, *31*, L06301, doi:10.1029/2003GL019018.

Conkright, M., et al. (1998), World Ocean Database 1998 Documentation and Quality Control, *NODC Internal Rep. 14*, Natl. Oceanogr. Data Cent., Silver Spring, Md.

Dandonneau, Y. (1971), Étude du phytoplancton sur le plateau continental de Côte d'Ivoire I. - Groupes d'espèces associées, *Cah. O.R.S.T.O.M., Ser. Oceanogr.*, *IX*, 247–265.

da Silva, A., A. C. Young, and S. Levitus (1994), *Atlas of Surface Marine Data 1994*, vol. 1, *Algorithms and Procedures*, *NOAA Atlas NESDIS 6*, Natl. Oceanic and Atmos. Admin., Silver Spring, Md.

Devassy, V. P. (1987), *Trichodesmium* red tides in the Arabian Sea, in *Contributions in Marine Sciences: A Special Volume to Felicitate Dr. S. Z. Qasim Sastyabdapūrtl on His Sixtieth Birthday*, edited by T. S. S. Rhao et al., pp. 61–66, Natl. Inst. of Oceanogr., Dona Paula, India.

Devassy, V. P., P. M. A. Bhattathiri, and S. Z. Qasim (1979), Succession of organisms following *Trichodesmium* phenomenon, *Ind. J. Mar. Sci.*, *8*, 89–93.

Dugdale, R. C., J. J. Goering, and J. H. Ryther (1964), High nitrogen fixation rates in the Sargasso Sea and the Arabian Sea, *Limnol. Oceanogr.*, *9*, 507–510.

Dunstan, W. M., and J. Hosford (1977), The distribution of planktonic blue green algae related to the hydrography of the Georgia Bight, *Bull. Mar. Sci.*, *27*, 824–829.

Goering, J. J., R. C. Dugdale, and D. Menzel (1966), Estimates of in situ rates of nitrogen uptake by *Trichodesmium* sp. in the tropical Atlantic Ocean, *Limnol. Oceanogr.*, *11*, 614–620.

Gruber, N., and J. L. Sarmiento (1997), Global patterns in marine nitrogen fixation and denitrification, *Global Biogeochem. Cycles*, *11*, 235–266.

Hernańdez-León, S., L. Postel, J. Arístegui, M. Gómez, M. Fernanda Montero, S. Torres, C. Almeida, E. Kuhner, U. Brenning, and E. Hagen (1999), Large-scale and mesoscale distribution of plankton biomass and metabolic activity in the northeastern Central Atlantic, *J. Oceanogr.*, *55*, 471–482.

Hood, R. R., A. E. Michaels, and D. G. Capone (2000), Answers sought to the enigma of marine nitrogen fixation, *Eos Trans. AGU*, *81*, 133, 138–139.

Hood, R. R., N. R. Bates, D. G. Capone, and D. B. Olson (2001), Modeling the effect of nitrogen fixation on carbon and nitrogen fluxes at BATS, *Deep Sea Res., Part II*, *48*, 1609–1648.

Hood, R. R., K. E. Kohler, J. P. McCreary, and S. Smith (2003), A 4-dimensional validation of a coupled physical-biological model of the Arabian Sea, *Deep Sea Res., Part II*, *50*, 2917–2945.

Hulburt, E. M. (1962), Phytoplankton in the southwestern Sargasso Sea and north Equatorial Current, February 1961, *Limnol. Oceanogr.*, *7*, 307–315.

Hulburt, E. M. (1968), Phytoplankton observations in the western Caribbean Sea, *Bull. Mar. Sci.*, *18*, 388–399.

Karl, D., R. Letelier, L. Tupas, J. Dore, J. Christian, and D. Hebel (1997), The role of nitrogen fixation in biogeochemical cycling in the subtropical North Pacific Ocean, *Nature*, *388*, 533–538.

Krauk, J. M. (2001), Plasticity and limits on N:P in *Trichodesmium* spp.: A comparison between field and cultured populations, M.S. thesis, 81 pp., Univ. of Md., College Park.

Kraus, E. B., and J. S. Turner (1967), A one-dimensional model of the seasonal thermocline: II. The general theory and its consequences, *Tellus*, *19*, 98–105.

Lenes, J. M., et al. (2001), Iron fertilization and the *Trichodesmium* response on the West Florida shelf, *Limnol. Oceanogr.*, *6*, 1261–1277.

Lipschultz, F., and N. J. P. Owens (1996), An assessment of nitrogen fixation as a source of nitrogen to the North Atlantic Ocean, *Biogeochemistry*, *35*, 261–274.

Mahadevan, A., and D. Archer (2000), Modeling the impact of fronts and mesoscale circulation on the nutrient supply and biogeochemistry of the upper ocean, *J. Geophys. Res.*, *105*, 1209–1225.

Margalef, R. (1963a), Succession in marine populations, in *Advancing Frontiers of Plant Sciences*, vol. 2, edited by R. Vira, pp. 137–188, Inst. for the Adv. of Sci. and Cult., Delhi.

Margalef, R. (1963b), Some concepts relative to the organization of plankton, *Oceanogr. Mar. Biol. Annu. Rev.*, *5*, 257–289.

Margalef, R. (1973), Fitoplancton marino del la región de afloramiento del NW de África: II. Composition y distribución del fitoplancton, *Res. Exp. Cient B/O Cornide*, *2*, 65–94.

McCreary, J. P., Jr., K. E. Kohler, R. R. Hood, and D. B. Olson (1996), A four-component ecosystem model of biological activity in the Arabian Sea, *Prog. Oceanogr.*, *37*, 193–240.

McCreary, J. P., Jr., K. E. Kohler, R. R. Hood, S. Smith, J. Kindle, A. S. Fischer, and R. A. Weller (2001), Influences of diurnal and intraseasonal forcing on mixed-layer and biological variability in the Arabian Sea, *J. Geophys. Res.*, *106*, 7139–7155.

McGillicuddy, D. J., and A. R. Robinson (1997), Eddy induced nutrient supply and new production in the Sargasso Sea, *Deep Sea Res., Part I*, *44*, 1427–1499.

McGillicuddy, D. J., A. R. Robinson, D. A. Siegel, H. W. Jannasch, R. J. Johnson, T. D. Dickey, J. McNeil, A. F. Michaels, and A. H. Knap (1998), Influence of mesoscale eddies on new production in the Sargasso Sea, *Nature*, *394*, 263–266.

Moore, J. K., S. C. Doney, J. A. Kleypas, D. M. Glover, and I. Y. Fung (2002), An intermediate complexity marine ecosystem model for the global domain, *Deep Sea Res., Part II*, *49*, 403–462.

Navarro, R. A. (1998), Optical properties of photosynthetic pigments and abundance of the cyanobacterium *Trichodesmium* in the eastern Caribbean basin, Ph.D. thesis, Univ. of Puerto Rico, Rio Piedras.

O'Neil, J. M. (1997), The colonial cyanobacterium *Trichodesmium* as a physical and nutritional substrate for the harpacticoid copepod *Macrosetella gracilis*, *J. Plankton Res.*, *20*, 43–59.

O'Neil, J. M., P. M. Metzler, and P. M. Glibert (1996), Ingestion of $^{15}N_2$-labeled *Trichodesmium* sp. and ammonium regeneration by the harpacticoid copepod *Macrosetella gracilis*, *Mar. Biol.*, *125*, 89–96.

Orcutt, K. M., F. J. Lipschultz, K. Gundersen, R. Arimoto, J. R. Gallon, A. F. Michaels, and A. H. Knap (2001), A seasonal study of the significance of N_2 fixation by *Trichodesmium* spp. at the Bermuda Atlantic Time-Series Study (BATS) site, *Deep Sea Res.*, *48*, 1583–1608.

O'Reilly, J. E., S. Maritorena, B. G. Mitchell, D. A. Siegel, K. L. Carder, S. A. Garver, M. Kahru, and C. McClain (1998), Ocean color chlorophyll algorithms for SeaWiFS, *J. Geophys. Res.*, *103*, 24,937–24,953.

Oschlies, A. (2000), Equatorial nutrient trapping in biogeochemical ocean models: The role of advection numerics, *Global Biogeochem. Cycles*, *14*, 655–667.

Oschlies, A., and V. Garcon (1999), An eddy-permitting coupled physical-biological model of the North Atlantic: 1. Sensitivity to physics and numerics, *Global Biogeochem. Cycles*, *13*, 135–160.

Paerl, H. W., L. E. Prufert-Bebout, and C. Gou (1994), Iron-stimulated N_2 fixation and growth in natural and cultured populations of the planktonic marine cyanobacteria *Trichodesmium* spp., *Appl. Environ. Microbiol.*, *60*, 1044–1047.

Revelante, N., W. T. Williams, and J. S. Bunt (1982), Temporal and spatial distributions of diatoms, dinoflagellates and *Trichodesmium* in waters of the Great Barrier Reef, *J. Exper. Mar. Biol. Ecol.*, *63*, 27–45.

Rueter, J. G. (1983), Theoretical iron limitation of microbial N_2 fixation in the oceans, *Eos Trans. AGU*, *63*, 445.

Rueter, J. G., D. A. Hutchins, R. W. Smith, and N. L. Unsworth (1992), Iron nutrition of *Trichodesmium*, in *Marine Pelagic Cyanobacteria:* Trichodesmium *and Other Diazotrophs*, edited by E. J. Carpenter, D. G. Capone, and J. G. Rueter, pp. 289–306, Kluwer Acad., Norwell, Mass.

Sander, F., and D. M. Steven (1973), Organic productivity of inshore and offshore waters of Barbados: A study of the island mass effect, *Bull. Mar. Sci.*, *23*, 771–792.

Sañudo-Wilhelmy, S. A., A. B. Kustka, C. J. Gobler, D. A. Hutchins, M. Yang, K. Lwiza, J. Burns, D. G. Capone, J. A. Raven, and E. J. Carpenter (2001), Phosphorus limitation of nitrogen fixation by *Trichodesmium* in the central Atlantic Ocean, *Nature*, *411*, 66–69.

Smolarkiewicz, P. K. (1983), A simple positive definite advection scheme with small implicit diffusion, *Mon. Weather Rev.*, *111*, 479–486.

Steven, D. M., and R. Glombitza (1972), Oscillatory variation of a phytoplankton population in a tropical ocean, *Nature*, *237*, 105–107.

Subramaniam, A., C. W. Brown, R. R. Hood, E. J. Carpenter, and D. G. Capone (2002), Detecting *Trichodesmium* blooms in SeaWiFS imagery, *Deep Sea Res., Part II*, *49*, 107–121.

Tyrrell, T., E. Marañón, A. Poulton, A. R. Bowie, D. S. Harbour, and E. M. S. Woodward (2003), Large-scale latitudinal distribution of *Trichodesmium* spp. in the Atlantic Ocean, *J. Plankton Res.*, *25*, 405–416.

Vallespinos, F. (1985), Nitrogen fixation by *Trichodesmium thiebautii* in the upwelling region off northwest Africa, in *Simposio Internacional sobre las Areas de Afloramiento Mas Important del Oeste Africano (Cabo Blanco Y Benguela)*, vol. 1, edited by C. Bas, R. Margalef, and P. Rubies, Inst. de Invest. Pesqueras Barcelona, Barcelona.

Vidal, M., C. Duarte, T. Granata, and S. Agusti (1999), Dissolved organic nitrogen and phosphorus pools and fluxes in the central Atlantic Ocean, *Limnol. Oceanogr.*, *44*, 106–115.

Walsh, J. J., and K. A. Steidinger (2001), Saharan dust and Florida red tides: The cyanophyte connection, *J. Geophys. Res.*, *106*, 11,597–11,612.

Wille, N. (1904), Die schizophyceen der plankton expedition, *Ergeb. Humbolt-Stift*, *4*, 1–88.

Wu, J., W. Sunda, E. A. Boyle, and D. M. Karl (2000), Phosphate depletion in the western North Atlantic Ocean, *Science*, *289*, 759–762.

Zehr, J. P., J. B. Waterbury, P. J. Turner, J. P. Montoya, E. Omoregie, G. F. Steward, A. Hansen, and D. M. Karl (2001), Unicellular cyanobacteria fix N_2 the subtropical North Pacific Ocean, *Nature*, *412*, 635–638.

D. G. Capone, Wrigley Institute for Environmental Studies and Department of Biological Sciences, University of Southern California, 3616 Trousdale Parkway, AHF 108, Los Angeles, CA 90089-0371, USA. (capone@wrigley.usc.edu)

V. J. Coles and R. R. Hood, Horn Point Laboratory, University of Maryland Center for Environmental Science, 2020 Horns Point Road, P.O. Box 775, Cambridge, MD 21613, USA. (raleigh@hpl.umces.edu)